USAAMRDL TECHNICAL REPORT 72-4

EXPERIMENTAL INVESTIGATION OF EFFECTS OF BLADE SECTION CAMBER AND PLANFORM TAPER ON ROTOR HOVER PERFORMANCE

By

E. Dean Bellinger

March 1972

EUSTIS DIRECTORATE
U. S. ARMY AIR MOBILITY RESEARCH AND DEVELOPMENT LABORATORY
FORT EUSTIS, VIRGINIA

CONTRACT DAAJ02-71-C-0012
UNITED AIRCRAFT CORPORATION RESEARCH LABORATORIES
EAST HARTFORD, CONNECTICUT

85

DISCLAIMERS

The findings in this report are not to be construed as an official Department of the Army position unless so designated by other authorized documents.

When Government drawings, specifications, or other data are used for any purpose other than in connection with a definitely related Government procurement operation, the United States Government thereby incurs no responsibility nor any obligation whatsoever; and the fact that the Government may have formulated, furnished, or in any way supplied the said drawings, specifications, or other data is not to be regarded by implication or otherwise as in any manner licensing the holder or any other person or corporation, or conveying any rights or permission, to manufacture, use, or sell any patented invention that may in any way be related thereto.

Trade names cited in this report do not constitute an official endorsement or approval of the use of such commercial hardware or software.

DISPOSITION INSTRUCTIONS

Destroy this report when no longer needed. Do not return it to the originator.

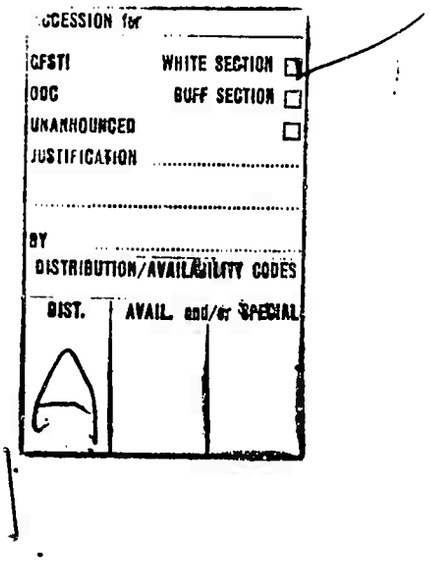

Unclassified
Security Classification

DOCUMENT CONTROL DATA - R & D

(Security classification of title, body of abstract and indexing annotation must be entered when the overall report is classified)

1. ORIGINATING ACTIVITY (Corporate author)	2a. REPORT SECURITY CLASSIFICATION
United Aircraft Corporation Research Laboratories East Hartford, Connecticut	Unclassified
	2b. GROUP

3. REPORT TITLE

EXPERIMENTAL INVESTIGATION OF EFFECTS OF BLADE SECTION CAMBER AND PLANFORM TAPER ON ROTOR HOVER PERFORMANCE

4. DESCRIPTIVE NOTES (Type of report and inclusive dates)

Final Report

5. AUTHOR(S) (First name, middle initial, last name)

E. Dean Bellinger

6. REPORT DATE	7a. TOTAL NO. OF PAGES	7b. NO. OF REFS
March 1972	83	10

8a. CONTRACT OR GRANT NO.	9a. ORIGINATOR'S REPORT NUMBER(S)
DAAJ02-71-C-0012 b. PROJECT NO.	USAAMRDL Technical Report 72-4
c. Task 1F162204AA4201	9b. OTHER REPORT NO(S) (Any other numbers that may be assigned this report)
d.	UARL K911076-14

10. DISTRIBUTION STATEMENT

Approved for public release; distribution unlimited.

11. SUPPLEMENTARY NOTES	12. SPONSORING MILITARY ACTIVITY
	Eustis Directorate U.S. Army Air Mobility R&D Laboratory Fort Eustis, Virginia

13. ABSTRACT

An experimental and analytical investigation was conducted to determine the effects of blade section camber and blade planform taper on helicopter rotor hover performance and to assess the accuracy of several theoretical methods in predicting such performance. The tests were conducted using small scale model rotors (nominally 4 feet in diameter) operating in and out of ground effect at full-scale tip speeds. The NACA 23112 airfoil, which is a section specifically designed to produce very low pitching moments such as required for helicopter blade applications, was selected for the cambered blade. A nominal taper ratio of 2:1 was selected for the tapered blade tests. The experimental results indicated a significant improvement in the maximum thrust capability of the cambered blade compared to blades having an NACA 0012 airfoil section. In addition, more efficient operation was achieved for the cambered blade at moderate thrust levels compared to the symmetrical blade. Blade taper increased rotor efficiency below stall but also reduced the rotor thrust level at which stall occurred. The earlier stall of the tapered blades is attributed to a greater interference of the blade tip region with the tip vortex from the preceding blade. The performance analyses based on the assumption of undistorted (i.e., uncontracted) wakes over-predicted rotor thrust for both the cambered and tapered blade rotors. However, improved performance prediction for the cambered blade rotor was achieved with a prescribed distorted wake analysis using symmetrical blade wake geometry data. These same wake geometry data, however, were found to be unreliable in predicting tapered blade performance, since, unlike camber, blade taper significantly influences wake geometry, and quantitative wake data defining this influence were not available for this investigation.

DD FORM 1 NOV 68 1473 REPLACES DD FORM 1473, 1 JAN 64, WHICH IS OBSOLETE FOR ARMY USE.

Unclassified
Security Classification

14. KEY WORDS	LINK A		LINK B		LINK C	
	ROLE	WT	ROLE	WT	ROLE	WT
Helicopter Rotors						
Helicopter Rotor Hover Performance						
Helicopter Rotor Wake						
Wake Geometry						
Vortices						
Hovering						
Helicopter Rotor Aerodynamics						
Helicopter Rotor Airloads						
Distorted Wake						
Model Tests						
Model Helicopter Rotor Tests						
Cambered Rotor Blades						
Tapered Rotor Blades						

DEPARTMENT OF THE ARMY
U. S. ARMY AIR MOBILITY RESEARCH & DEVELOPMENT LABORATORY
EUSTIS DIRECTORATE
FORT EUSTIS, VIRGINIA 23604

This report has been reviewed by the Eustis Directorate, U. S. Army Air Mobility Research and Development Laboratory, and is considered to be technically sound. This program was initiated to conduct an experimental investigation to determine the effects of blade section camber and blade planform taper on rotor hover performance. The principal objectives of this investigation were (1) to conduct tests to measure the hover performance of rotors with cambered and tapered blades as functions of number of blades, tip Mach number, and thrust, and (2) to evaluate the accuracy of various theoretical methods to predict hover performance of rotors with blade section camber and planform taper.

The report is published for the exchange of information and the stimulation of ideas.

The program was conducted under the technical management of Mr. William T. Yeager, Jr., and Mr. G. Thomas White of the Aeromechanics Division of this Directorate.

Task 1F162204AA4201
Contract DAAJ02-71-C-0012
USAAMRDL Technical Report 72-4
March 1972

EXPERIMENTAL INVESTIGATION OF EFFECTS OF BLADE SECTION CAMBER AND PLANFORM TAPER ON ROTOR HOVER PERFORMANCE

UARL K911076-14

by

E. Dean Bellinger

Prepared by

United Aircraft Corporation
Research Laboratories
East Hartford, Connecticut

for

EUSTIS DIRECTORATE
U. S. ARMY AIR MOBILITY RESEARCH AND DEVELOPMENT LABORATORY
FORT EUSTIS, VIRGINIA

SUMMARY

An experimental and analytical investigation was conducted to determine the effects of blade section camber and blade planform taper on helicopter rotor hover performance and to assess the accuracy of several theoretical methods in predicting such performance. The tests were conducted using small scale model rotors (nominally 4 feet in diameter) operating in and out of ground effect at full-scale tip speeds. The NACA 23112 airfoil, which is a section specifically designed to produce very low pitching moments such as required for helicopter blade applications, was selected for the cambered blade. A nominal taper ratio of 2:1 was selected for the tapered blade tests. The experimental results indicated a significant improvement in the maximum thrust capability of the cambered blade compared to blades having an NACA 0012 airfoil section. In addition, more efficient operation was achieved for the cambered blade at moderate thrust levels compared to the symmetrical blade. Blade taper increased rotor efficiency below stall but also reduced the rotor thrust level at which stall occurred. The earlier stall of the tapered blades is attributed to a greater interference of the blade tip region with the tip vortex from the preceding blade. The performance analyses based on the assumption of undistorted (i.e., uncontracted) wakes over-predicted rotor thrust for both the cambered and tapered blade rotors. However, improved performance prediction for the cambered blade rotor was achieved with a prescribed distorted wake analysis using symmetrical blade wake geometry data. These same wake geometry data, however, were found to be unreliable in predicting tapered blade performance, since, unlike camber, blade taper significantly influences wake geometry, and quantitative wake data defining this influence were not available for this investigation.

FOREWORD

This investigation was sponsored by the U. S. Army Air Mobility Research and Development Laboratory, Eustis Directorate, under Contract DAAJ02-71-C-0012, Task 1F162204AA4201. Efforts under this contract were initiated in October 1970 and completed in October 1971. The experimental program reported herein was conducted during the period February to April 1971.

The technical representatives of the Contracting Officer for this contract were Mr. William T. Yeager, Jr., and Mr. G. Thomas White of the Eustis Directorate.

TABLE OF CONTENTS

LIST OF ILLUSTRATIONS

LIST OF TABLES

LIST OF SYMBOLS

AR	Blade aspect ratio, c/R
b	Number of blades
c	Blade chord at 0.75 R, ft
c_d	Section drag coefficient
c_ℓ	Section lift coefficient
C_T	Rotor thrust coefficient, $T/\rho\pi R^2(\Omega R)^2$
C_Q	Rotor torque coefficient, $Q/\rho\pi R^2(\Omega R)^2$
k_1	Average axial velocity of tip vortex element from the time at which it was shed by a given blade to the time it passes the following blade, nondimensionalized by ΩR
M	Local blade section Mach number
Q	Rotor torque, ft-lb
Q_i	Induced rotor torque, ft-lb
Q_p	Profile rotor torque, ft-lb
$\bar{r}$	Distance from rotor axis of rotation to blade section or wake vortex element, measured parallel to plane of rotation and nondimensionalized by R
R	Rotor radius, ft
T	Rotor thrust, lb
V_z	Induced velocity at blade in axial direction, ft/sec
x	Axis parallel to blade chord, ft
y	Axis perpendicular to blade chord, ft

$\bar{z}$	Axial coordinate parallel to shaft axis of rotation and nondimensionalized by R, positive in direction of rotor thrust
z_G	Distance between the center of the rotor hub and the simulated ground, ft
α	Section angle of attack, deg
Γ	Local blade circulation (equal to $\Omega R \bar{r} c c_\ell/2$), or strength of vortex element in wake, ft^2/sec
$\Delta\psi_w$	Increment in wake azimuth angle, deg or rad
θ_1	Rate of change of local blade pitch angle due to built-in linear twist with respect to blade spanwise direction, positive when tip section is twisted leading-edge up relative to root section, deg
θ_{75}	Blade collective pitch as measured at the 0.75 R station, deg
ρ	Air density, $lb\text{-}sec^2/ft^4$
σ	Rotor solidity, ratio of total blade area to disc area, $bc/\pi R$
ψ_w	Wake element azimuth angle measured from blade, deg
Ω	Rotor rotational frequency, rad/sec

Subscripts

IGE	Denotes quantity evaluated in ground effect
max	Denotes maximum value of quantity
OGE	Denotes quantity evaluated out of ground effect

INTRODUCTION

An investigation was previously conducted at the United Aircraft Research Laboratories (UARL) under Army sponsorship in which the effects of number of blades, blade twist, blade aspect ratio, tip speed, and collective pitch on hover performance were measured for model helicopter rotors having untapered blades with symmetrical airfoil sections[1]. The objective of the investigation reported herein was to extend these tests to include the effects of two additional parameters which were expected to have a significant influence on performance. These parameters were blade camber and planform taper. Hover performance data were obtained using test equipment and model fabrication methods identical to those of Reference 1 and thereby providing a more complete body of extensive, self-consistent experimental data quantifying the effects of primary helicopter rotor design parameters.

An additional objective of this study was to evaluate the accuracy of several hover performance methods in predicting the effects of camber and taper on hover performance. These included both undistorted wake analyses and a UARL-developed prescribed wake analysis using distorted wake geometry data.

EXPERIMENTAL PROGRAM

TEST EQUIPMENT

Model Test Facility

The test program was conducted in the model rotor hover test facility located at the United Aircraft Research Laboratories (UARL). The test facility, shown in Figure 1, consists of a large enclosed area approximately 45 by 55 feet with a ceiling height of 40 feet. The facility is equipped with a rotor test rig, flow visualization equipment, and a movable ground plane to simulate in-ground-effect operation.

The model rotor test rig is shown in Figure 2. A 40-horsepower, variable-speed electric motor was used as a power source, and the rotor was driven through a 3:1 speed reduction system to allow operation at a tip speed of 700 feet/second at maximum available power. Average rotor thrust and torque measurements were obtained through strain-gaged load cells mounted on the rotor support frame. The motor-balance assembly is shown schematically in Figure 3. Additional instrumentation, used to monitor operation, included a solid-state counter for measuring rpm, vibration meters, and a model power control console.

Flow visualization data were taken for selected flight conditions; a description of the equipment and procedures is given in Reference 1.

Model Rotors

The model rotor system consisted of a multibladed rotor hub and specially designed model blades. The rotor hub, shown in Figure 4, was designed to accommodate any number of blades up to and including eight. Flapping hinges were provided (but no lag hinges), and blade collective pitch was varied manually. The model blade consisted of an aluminum spar and a balsa trailing-edge section, as shown in Figure 5. The blades were untwisted and designed such that the elastic axis and section center of gravity were coincident at the quarter-chord position (within 1 percent of the chord). The mass and stiffness properties of the model blades greatly exceeded those of model blades dynamically scaled from typical full-scale designs. For example, the Lock number when operating at 700 feet/second tip speed was approximately 3, whereas the Lock number of a full-scale blade of similar aspect ratio (18.2) is typically 10. Hence, model blade coning angles were lower than full-scale coning angles.

However, the testing of such rotor blades has permitted concentration on the aerodynamic, rather than aeroelastic, aspects of rotor hover performance. The blade parameters are summarized in Table I.

TABLE I. MODEL ROTOR BLADE PARAMETERS

Blade Parameter	Design 1	Design 2	Design 3
Linear Twist, θ_1, (deg)	0	0	0
Aspect Ratio, AR	18.2	18.2	18.2*
Radius, R (in.)	26.75	26.75	26.75
Chord, c (in.)	1.47	1.47	1.47**
NACA Airfoil Section	0012	23112	0012
Taper Ratio (root chord/tip chord)	1:1	1:1	2:1
Root Cutout (% R)	14.8	14.8	14.8
Flapping Hinge Offset (% R)	6.8	6.8	6.8

*Aspect ratio is based on the 0.75 R chord.
**Chord at the 0.75 R station.

Design 1 (untapered, symmetrical blades) was fabricated and performance tested by United Aircraft under Contract DAAJ02-69-C-0056 prior to this investigation. However, additional in-ground-effect performance data for this design were obtained during this investigation. The remaining two blade designs (Designs 2 and 3, referred to as cambered and tapered blades, respectively) were constructed specifically for this investigation. The airfoil profile coordinates nondimensionalized by chord are listed in Table II, and photographs of the two blades are shown in Figure 6. The NACA 23112 airfoil[2] was selected for the cambered blade for this investigation. This airfoil is desirable for helicopter application since it achieves high lift coefficients typical of cambered airfoils while producing nominally zero pitching moments.

TABLE II. AIRFOIL PROFILE COORDINATES

Cambered Airfoil NACA 23112			Tapered Airfoil NACA 0012		
x/c	y/c_{upper}	y/c_{lower}	x/c	y/c_{upper}	y/c_{lower}
0	0	0	0	0	0
0.0125	0.0276	-0.0119	0.0050	-	-
0.025	0.0372	-0.0167	0.0125	0.01894	-0.01894
0.050	0.0507	-0.0211	0.025	0.02615	-0.02615
0.075	0.0601	-0.0245	0.050	0.03555	-0.03555
0.100	0.0665	-0.0272	0.075	0.04200	-0.04200
0.15	0.0743	-0.0326	0.10	0.04683	-0.04683
0.20	0.0771	-0.0377	0.15	0.05345	-0.05345
0.25	0.0774	-0.0413	0.20	0.05738	-0.05738
0.30	0.0764	-0.0437	0.25	0.05941	-0.05941
0.40	0.0710	-0.0452	0.30	0.06002	-0.06002
0.50	0.0628	-0.0433	0.40	0.05803	-0.05803
0.60	0.0525	-0.0390	0.50	0.05294	-0.05294
0.70	0.0408	-0.0323	0.60	0.04563	-0.04563
0.80	0.0285	-0.0242	0.70	0.03664	-0.03664
0.90	0.0152	-0.0139	0.80	0.02623	-0.02623
0.95	0.0083	-0.0078	0.90	0.01448	-0.01448
1.00	0.0013	-0.0013	0.95	0.00807	-0.00807
			1.00	0.00126	-0.00126
Leading edge radius/c = 0.0158					

Each rotor was tested with the following numbers of blades and rotor solidities:

Number of Blades, b	Rotor Solidity, σ (based on c at 0.75 R)
2	0.035
4	0.070
6	0.105
8	0.140

TEST PROCEDURES

Calibration

The thrust and torque calibration derivatives were determined directly in strain gage units per pound (SGU/lb) and strain gage units per foot-pound (SGU/ft-lb), respectively, by applying known forces and moments to the rotor hub.

A dowel pin, mounted perpendicular to an arm extending from the root of the blade along the blade chord (see Figure 4), was used to manually set collective pitch angle relative to a flat surface on the blade retention fitting (attached to the hub). For each blade, the distance from the pin to the flat surface, measured by means of a depth micrometer, was calibrated relative to the collective pitch at the three-quarter radius. Blade tracking was checked by observing the blade tips through a transit, with lighting supplied by a strobotac triggered at a specified number of flashes per rotor revolution. In this manner, several blades were observed at once and their relative tip positions compared.

Test Parameters

Experimental data were systematically obtained to measure the effect of the following parameters on hover performance for rotors with blade section camber and planform taper. Reference data were obtained for a conventional rotor having untapered, symmetrical blades at 6 and 10 degrees collective pitch. The additional data presented herein for operating out of ground effect were obtained from Reference 1.

Primary Test Parameter	Nominal Test Values
1. Number of Blades, b	2, 4, 6, 8
2. Rotor Tip Speed, ΩR	525, 600, 700 fps
3. Collective Pitch, θ_{75}	0 to max*, deg
4. Height Above Ground/Rotor Radius, Z_G/R	3.5, 2.0, 1.33, 0.67

*Determined by operating stall limits.

Variations of the first three primary test parameters were equivalent to independent variations in three related parameters. That is, variations in number of blades were equivalent to variations in rotor solidity. Tip speed values of 525, 600, and 700 feet/second corresponded to tip Mach numbers of 0.46, 0.53, and 0.63, respectively. Finally, variations in

collective pitch were used to produce major variations in rotor thrust level. Five values of collective pitch (nominal values were 0, 6, 8, 10, 11 degrees for Designs 1 and 3, and -2, 4, 6, 8, 9 degrees for Design 2) were selected to span the thrust level from zero to maximum thrust. As a precautionary measure, the preliminary maximum collective pitch was selected so that all the required data were obtained before more extensive data, specifically in the stall region, were taken. As indicated by the above listing of parameters, data regarding the effect of rotor height above the ground was investigated for rotors using three blade designs. A rotor height ratio (distance above the ground to rotor radius) of 3.5 simulated out of ground effect operation while ratios of 2.0, 1.33, and 0.67 simulated various levels of in ground effect operation.

Test Configuration

The test parameter combinations that were investigated are listed in Table III. The untapered blade rotor having an NACA 0012 airfoil will hereafter be referred to as the "reference rotor".

TABLE III. TEST PARAMETER COMBINATIONS

Blade Airfoil Section	Taper Ratio	Rotor Condition	Height Above Ground/ Rotor Radius	No. of Blades	No. of Tip Speeds	No. of Collective Pitch Values
NACA 23112	1:1	OGE	3.5	2,4,6,8	3	5*
NACA 0012	2:1	OGE	3.5	2,4,6,8	3	5*
NACA 0012	1:1	OGE	3.5	4,6,8	2	2
NACA 23112	1:1	IGE	2.0,1.33,0.67	4,6,8	2	2
NACA 0012	2:1	IGE	2.0,1.33,0.67	4,6,8	2	2
NACA 0012	1:1	IGE	2.0,1.33,0.67	4,6,8	2	2
NACA 0012**	1:1	OGE	3.5	2,4,6,8	3	5*

*Minimum number.
**Performance results obtained from previous investigation.

The hover performance for the combination of parameters presented as the last item in Table III were obtained from tests conducted as part of the experimental investigation reported in Reference 1.

Data Acquisition

The procedure for data acquisition fundamentally consisted of selecting the test configuration (blade design, collective pitch, ground-plane position, and number of blades) and recording performance data at the required tip speeds. The ambient temperature and pressure in the enclosed area were monitored and recorded during the test. The rotor thrust and torque data were acquired by manually recording the outputs of the thrust and torque load cells on self-balancing potentiometers in strain gage units (SGU). Oscillations of the potentiometer readings as high as ±10 SGU (±0.3 lb) for thrust and ±30 SGU (±0.2 ft-lb) for torque were observed for some test conditions. To establish representative steady-state values, average readings were recorded. The repeatability of the data was determined as described in Reference 1.

For most rotor configurations, the maximum collective pitch at which operation was possible was limited by the occurrence of a sharp increase in rotor noise level as the tip speed was increased beyond a certain level. This boundary was explored during the tests of Reference 1 and was found to be related to stall flutter. The reference and cambered blade designs indicated a sharp transition to a higher rotor noise level at the stall flutter boundary; however, the tapered blade did not indicate a distinct stall flutter boundary. The noise level for this rotor indicated a gradual transition from normal operating noise to a steady and relatively intense noise level. It was this steady and intense noise level which was defined to be the boundary for maximum thrust.

Flow visualization was not an objective of this test; however, to obtain a sampling for comparison with the reference rotor, data were obtained for three hover conditions with six-bladed rotors operating at 600 feet/second tip speed out of ground effect. Flow visualization data were obtained for cambered blades at two thrust levels (C_T/σ = 0.0281 and 0.1015) and for tapered blades at one thrust level (C_T/σ = 0.0433). The tip vortex positions are shown in Figure 7 for the cambered blades at C_T/σ = 0.0281 and for the tapered blades at C_T/σ = 0.0433 and are compared to those of the reference rotor at C_T/σ = 0.0300. The apparent difference of the blade azimuth spacing for the reference rotor shown in Figure 7c is due to a different camera mounting position. This rotor was photographed earlier under another investigation[1].

TEST DATA ACCURACY

Static data repeatability for thrust and torque was determined from repeated calibrations of the strain gages while determining the calibration derivatives discussed in the Test Procedures section. The repeatability values are listed below as two standard deviations:

	Thrust, lb	Torque, ft-lb
Static Data Repeatability:	± 0.131	± 0.120

The dynamic data repeatability was determined by considering the range of C_T/σ and C_Q/σ from average values calculated from repeated test points during a test run. Either two or three repeated data points were recorded during a run, where a test run consisted of test data recorded between the starting and stopping of the rotor. A mean range was calculated for all the conditions with repeated data, and the averages are listed below:

	Average	
	C_T/σ	C_Q/σ
Dynamic Data Repeatability:	± 0.00015	± 0.000024

The quoted values do not reflect scatter due to any differences in setting collective pitch. The differences due to any errors in setting collective pitch were significant, but they had very little influence on the rotor thrust-torque relations, as will be shown in the presentation of the performance results.

The estimated accuracies with which the parameters determining a given test condition could be set are given below:

Parameter	Accuracy
Collective Pitch, θ_{75}	± 0.2 deg
Tip Speed, ΩR	± 1 fps
Rotor Height, Z_G/R	± 0.03

DISCUSSION OF EXPERIMENTAL ROTOR PERFORMANCE RESULTS

All experimental results are presented in graphical form in Figures 8 through 17 to demonstrate the influence of blade camber and taper for various combinations of number of blades (solidity), tip speed, and simulated ground height. Figures 8 through 10 present the basic performance characteristics (out of ground effect) of the reference rotor (symmetrical airfoil, no taper) and the rotor having cambered and tapered blades. The data for the reference rotor (Figure 8) was obtained from Reference 1; however, additional data for the reference rotors with 4, 6, and 8 blades were also obtained during this test program to verify the Reference 1 results. The influence of collective pitch, number of blades, tip speed, camber, and taper are shown in Figures 11 through 15. The experimental data points have been removed from Figures 11 through 15 for clarity, and the faired curves are presented for discussion purposes. Finally, performance characteristics in ground effect are presented in Figures 16 and 17 for the three rotor systems. The results are discussed in the following paragraphs.

Thrust Limits

As noted previously, the maximum thrust (collective pitch) was limited for untapered and cambered rotor configurations by the occurrence of a sharp increase in rotor noise level as tip speed was increased. The exact nature of this boundary is not known but as discussed in Reference 1 may be related to incipient stall flutter triggered by blade-vortex interference. For this investigation the boundary was defined qualitatively by the test engineer during the test. The boundary was easily defined for the reference and cambered blades; however, it was more difficult to establish for the tapered blades. The noise level for the tapered blades at a specific collective pitch setting grew gradually with increasing thrust (through increasing tip speed), and testing was terminated when the noise level was judged to be as intense as that for the other rotors. Any uncertainties for this rotor due to this procedure were, fortunately, of little consequence since rotor torque data showed clear evidence of stall long before the noise limit dictated termination of the tests. Thus the physically interesting thrust range was covered for all rotors tested.

Using the above procedures, it was generally found that the maximum thrust was reduced as the tip speed increased (e.g., compare Figures 8a, 8b, and 8c). Furthermore, the cambered blade flutter boundary was above the untapered, symmetrical and tapered blade boundaries as a result of

the higher $c_{\ell_{max}}$ of the cambered airfoil (e.g., compare Figures 8a, 9a, and 10a). The lowest boundary occurred with the tapered blade, apparently as a result of early tip stall (see Figures 8a and 10a). The occurrence of such stall is related to blade-vortex interference which is evident from the flow visualization photographs of Figure 7. When comparing the positions of the tip vortex relative to the following blade, it can be seen that the cambered blade vortex has a greater vertical displacement than that for the tapered blade vortex. The tapered blade vortex actually impinges on the following blade and thus induces high angles of attack causing local stalling. The close proximity of the vortex is attributed to the reduced outboard blade area resulting in lower induced axial transport velocities.

Effect of Collective Pitch

The performance results are presented in Figures 8 through 10 in terms of rotor thrust versus torque to minimize the scatter introduced by any variations in setting the collective pitch, θ_{75}. Nominal values of collective pitch are indicated by the dashed lines in each figure. In addition, Figure 11 shows representative C_T/σ and C_Q/σ variations with collective pitch, θ_{75}. The results shown in Figure 11 correspond to the faired cambered and tapered blade data of Figures 9b and 10b, respectively. As anticipated, rotor torque increases rapidly at the higher collective pitch settings due to the divergence of the airfoil drag characteristics. The cambered blade data in Figure 11a indicate a reduction of slope, or falling-off, of lift at the high collective pitch settings for b = 2, 4, and 6. The slope reduction is even more pronounced for the tapered blade data shown in Figure 11b, indicating that the rotors were indeed operating with portions of the blades stalled.

Effect of Solidity and Number of Blades

Rotor solidity was changed, for each blade design, by varying the number of blades from 2 through 8, as indicated in Figures 8 through 10. Since each of the figures represents rotors with fixed blade chord distribution, radius, and tip speed, C_T/σ and C_Q/σ are directly related to the thrust and torque per blade (blade thrust and torque loading). Comparison of the results for varying numbers of blades within each figure indicates improved blade efficiency (thrust/blade (C_T/σ) per torque/blade (C_Q/σ)) with decreasing solidity. The improved blade efficiency is produced from two sources. First, and most important, the fewer number of blades (or lower solidity) at a given blade loading will produce a lower total thrust and disc loading of the rotor. As a result, the average

downwash (which is a measure of the energy expended) induced by the rotor wake will be lower and, hence, the blade induced drag will be less. A second smaller effect (discussed in Reference 1) arises from the local interference caused by the tip vortex shed from one blade on the loading of the following blade.

Although lower solidity at constant blade aspect ratio implies greater blade efficiency, a limit exists to which it also implies greater rotor efficiency. This is because of blade stall. Plots representing typical total rotor performance coefficients (C_T and C_Q) for rotors with cambered and tapered blades are given in Figures 12a and 12b, and correspond to the test conditions shown in Figures 9b and 10b, respectively. Since the blade radius and tip speed are constant in Figure 12, C_T and C_Q are proportional to the total rotor thrust and torque. Both Figures 12a and 12b show that the rotor thrust per unit rotor torque can be improved by decreasing solidity (blade area) until blade stall occurs.

Effect of Tip Speed

The influence of rotor tip speed (test values were 525, 600, and 700 feet/second) on hover performance is presented in Figure 13a for the cambered blades and in Figure 13b for the tapered blades. Both figures show the faired test data for 2- and 6-bladed rotor configurations. The test tip speeds at 525, 600, and 700 feet/second correspond to tip Mach numbers of 0.46, 0.53, and 0.63, respectively. Generally, an increase of the tip speed causes an increase in the rotor torque due to compressibility effects at constant thrust values, and the effect becomes more pronounced with increasing thrust and increasing tip speed.

Effect of Blade Section Camber

The relative influence on performance due to camber is shown in Figure 14. The faired curves through the performance data (from Figure 9) are again used to compare rotor performance. Representative results are shown in Figure 14 for 2- and 6-bladed cambered rotors and are compared to the reference rotor (symmetrical airfoil) data taken from Figure 8b. The results indicate an improvement in efficiency of approximately 6 percent for the cambered blades at the thrust level where the reference rotor stalls and a significant extension of the maximum thrust capability. The end points on the curves of Figure 14 (and 15) represent the stall boundary.

The higher torque requirement of the cambered blades at zero thrust indicated on Figure 14 is consistent with the higher drag of two-dimensional cambered sections at zero lift coefficient.

Effect of Blade Planform Taper

Representative effects of blade taper are shown in Figure 15 for 2- and 6-bladed rotors. The solid lines represent the faired curves through the tapered blade data of Figure 10b, and the dashed lines represent the faired curves through the reference rotor (untapered blade) data of Figure 8b. The results indicate an improvement in hover performance of approximately 5 percent for the tapered blades at moderate thrust coefficients. This would be expected due to the more uniform downwash distribution produced by the taper. However, as thrust is increased, blade stall occurs sooner for the tapered blade (discussed in the Thrust Limits section), and its thrust-torque relationship takes on a typical torque divergence character. The most significant aspect revealed by this investigation relative to tapered blades is the problem of blade-vortex interference. This has been shown by both the photographic information of Figure 7 and the noise level performance results to be a more serious problem than with conventional untapered blades. The reduced blade tip area, by virtue of the blade taper, develops a lower tip circulation strength, thereby reducing the primary factor which imparts the downward motion of the tip vortex. A similar effect would be caused if blade twist were introduced on an untapered blade due to the reduction in tip angle of attack as was demonstrated in Reference 1. However, because of its lower tip angles, the twisted blade is more tolerant of the upwash induced by the tip vortex, and its performance is not adversely affected. The results of such vortex interference on the tapered blade not only reduce its performance at high thrust levels but also can produce dynamic blade-out-of-track (BOOT) phenomena. BOOT was not experienced during the model tests since the blades were significantly stiffer than dynamically scaled blades and, therefore, were restricted in their response characteristics.

Ground Effect

As part of these tests, a systematic investigation of the in-ground-effect (IGE) performance for the three blade designs was conducted with various combinations of tip speed, number of blades, ground-plane height, and collective pitch. Tip speeds of 525 and 700 feet/second were selected for 4-, 6-, and 8-bladed rotors. The relative position of the rotor with respect to the ground was varied from 3.5 R, which is essentially out of ground effect (OGE), to 0.67 R, which is well within

ground effect. The rotor configuration and collective pitch setting were held fixed during the series of simulated rotor height variations. The effect of rotor height above ground on the rotor performance coefficients is shown in Figure 16 for the three blade designs with 6-bladed rotors operating at 700 feet/second tip speed. As demonstrated by the typical results in Figure 16, the variation of thrust with torque is essentially linear as the rotor height is varied.

Thrust augmentation is normally defined as the ratio of IGE thrust to OGE thrust at constant torque, as represented by the following equation:

$$\frac{T_{IGE}}{T_{OGE}} = \left[\frac{(C_T/\sigma)_{IGE}}{(C_T/\sigma)_{OGE}}\right]_{\text{CONSTANT } C_Q/\sigma}$$

The IGE data for the three blade designs are presented in Figure 17. It can be observed that the data (except for differences due to scatter) are generally independent of blade solidity (corresponding to 4, 6, and 8 blades) and variations in the OGE thrust level (corresponding to approximate collective pitch values of 6, 8, and 10 degrees). The thrust at the minimum rotor height was increased approximately 20 percent for each rotor over the thrust developed by operating OGE. Slight increases of thrust augmentation appear with increasing tip speed; however, no clear improvement in-ground-effect performance is distinguishable between the untapered, tapered, and cambered blades.

THEORETICAL METHODS FOR PREDICTING HOVER PERFORMANCE

An objective of this investigation was to evaluate the accuracy of certain theoretical methods, including two developed at UARL, in predicting the performance of rotors having cambered and tapered blades. The methods used for analysis are listed below:

1. Blade Element-Momentum Analysis
2. Goldstein-Lock Analysis
3. Prescribed Classical Wake Analysis
4. Prescribed Distorted Wake Analysis

Each method is described below, with emphasis placed on the last two, since the first two methods have been in widespread use for many years. The four methods are identical to the analyses employed for the investigation of Reference 1. In Reference 1, the Prescribed Distorted Wake Analysis was termed the Prescribed Experimental Wake Analysis.

The operating conditions for which rotor performance was computed are listed in Table IV.

TABLE IV. OPERATING CONDITIONS ANALYZED

Rotor	Airfoil	Taper Ratio	Twist (deg)	Aspect Ratio	No. of Blades	Tip Speed (fps)	Collective Pitch (deg)
Model	NACA 23112	1:1	0	18.2	6	600	4*,6,8,9*,10,11, 12,13*
Model	NACA 0012	2:1	0	18.2**	6	600	0.7*,4.7*,6.7, 8.7,10.7,11.7
Full-Scale	Sikorsky Cambered Airfoil	1:1	Non-linear, -10.6	15.1	6	698	12.9

All conditions investigated correspond to OGE operation.
*Conditions calculated with Blade Element-Momentum and Golstein-Lock Methods only.
**Based on the chord at 0.75 R.

BLADE ELEMENT-MOMENTUM ANALYSIS

This analysis is based on the assumption that the lift acting on an annulus of the rotor disc is equal to the change in momentum of the air passing through that annulus. Each annulus or, equivalently, each blade section is assumed to operate independently of all other sections. The relations developed can be shown (Heyson[3]) to be equivalent to those obtained using vortex theory in which the rotor is modeled by an infinite number of blades and the vorticity deposited in the wake of the rotor forms a continuous cylindrical vortex sheet having a diameter equal to the rotor diameter. The equations relating local blade thrust and local induced velocity at the disc are solved iteratively on a digital computer using appropriate two-dimensional airfoil data to account for any stall or compressibility effects that may be present. Losses due to flow around the tips of the blades are accounted for by specifying a "tip loss factor", which assumes complete loss of lift over a small, arbitrary percentage of the blade tip region. As used herein, the parameters specified as input to the analysis were rotor radius, solidity, blade chord, tip speed, blade twist, collective pitch, blade coning angle, air density, speed of sound, airfoil c_ℓ and c_d data, and tip loss factor (0.97).

In summary, the Blade Element-Momentum Analysis neglects effects due to the finite number of blades as well as those related to wake contraction.

GOLDSTEIN-LOCK ANALYSIS

This analysis is effectively the rotary-wing equivalent of the classical lifting-line analysis used successfully for fixed wings. The analysis is based principally on the work of Goldstein[4], who obtained a solution for the velocity potential for the flow about an axially translating, doubly-infinite, rigid helicoidal surface. This surface was shown by Betz[5] to represent the minimum energy wake of a propeller (or rotor) having a finite number of blades. By satisfying the flow boundary conditions on the helical surfaces representing the wake, the optimum (or Goldstein) distribution of circulation in the wake was obtained. Goldstein's results were applied by Lock[6], who showed how the results could be used to design a propeller. This was accomplished by assuming the propeller to be lightly loaded so that the wake was essentially uncontracted, in which case the circulation distribution in the wake can be related directly to the circulation distribution on the blade. Through this assumption and the use of the Goldstein velocity potential to define the induced velocities at the plane of the propeller, the blade twist and

chord distributions necessary to produce the Goldstein (optimum) circulation can be determined. Lock also postulated techniques for handling the inverse problem, wherein the blade geometry is defined and the circulation distribution and the associated propeller performance are required. This situation arises, for example, when one designs an optimum propeller for operation at a specified design condition and then wishes to know the performance of this propeller at off-design operating conditions. In his approach, Lock assumed that the circulation at each blade section was part of a Goldstein optimum circulation distribution but allowed the optimum distribution associated with each section to be different. This implies a different wake pitch angle variation with radius than would be the case for a blade whose local circulation values formed part of the same optimum distribution. The resulting wake structure is, therefore, technically inconsistent with the optimum wake assumptions made by Goldstein; however, reasonable answers are expected for conditions where large departures from the Goldstein optimum circulation distribution are not involved. Numerical implementation of the Goldstein-Lock method, which involves an iteration at each blade section between the local circulation and local wake pitch angle, was accomplished using an existing computer program provided by the Sikorsky Division.

In summary, the Goldstein-Lock Analysis accounts for the finite number of blades on a rotor (thereby eliminating the need for fictitious tip loss factors) but still retains the assumptions that the blades are lifting lines and that the wake is uncontracted (light loading).

UARL PRESCRIBED WAKE HOVER PERFORMANCE PROGRAM

The next two analyses to be discussed employ the UARL Prescribed Wake Hover Performance Program (or briefly, the Prescribed Wake Program) for the solution of the blade circulation and inflow distribution and the corresponding integrated rotor performance. Complete generality (within the framework of the assumptions to be mentioned) regarding the specification of the geometry of the wake was maintained in the computer program. This generality permits the evaluation of a wide variety of wake geometries such as a classical undistorted wake geometry (hereafter referred to as the classical wake), or a realistic model of a distorted wake. The incorporation of these two wake models in the Prescribed Wake Program results in the analyses listed below:

1. Prescribed Classical Wake Analysis
2. Prescribed Distorted Wake Analysis

These analyses are identical except for the representation of the wake. A description of the wake model used in each will be presented in the following sections. Other than assumptions regarding wake shape, the following are the major assumptions that currently exist in the Prescribed Wake Program:

1. Each blade is represented by a lifting line (bound vortex) divided into a finite number of segments (blade segments), each having a different circulation strength. The aerodynamic characteristics determined at the centers of each segment are assumed to be representative of the entire segment.

2. The wake is represented by a finite number of vortex filaments trailing from the blade segment boundaries. Each filament is divided into straight segments, the lengths of which are determined by a specified wake azimuth interval, $\Delta\psi_w$. The circulation strength of each trailing vortex filament is constant along its length and is equivalent to the difference between the circulation values of its adjacent bound vortex segments in accordance with Helmholtz laws of conservation of vorticity.

3. The blade and wake characteristics are assumed to be independent of azimuth position.

4. The airflow at the blades is assumed to be two-dimensional (radial induced velocity components are neglected). For the rotor performance calculations, tabulated two-dimensional airfoil data (c_ℓ, c_d, α) are provided which include compressibility effects (Mach number variations). For the circulation calculations, a set of lift curve slopes and stall angles of attack are provided which vary with each Mach number.

5. Tangential induced velocity components are neglected.

6. Small-angle assumptions are included for the inflow angles in the circulation solution.

7. Following the blade circulation and inflow solution, conventional strip theory is assumed to be applicable to compute the rotor performance characteristics.

The method differs from that developed by Rorke and Wells[7] in that the blade inflow distribution is determined completely by the induced effects of the wake (by application of the Biot-Savart law) as opposed to introducing approximate momentum considerations. A flow diagram showing the required input, sequence of major operations, and output of the program is presented in Figure 18. As indicated in this figure, the program is divided into three independent parts. The first transforms the wake geometry input to wake coordinates. The second contains the computation of the wake influence coefficients at the blade, as defined by the Biot-Savart law, and the numerical procedure for solving the circulation matrix and associated induced velocity distribution. In the third part, performance characteristics are computed. A provision for automatic plotting of the wake filaments is included. Sample computer plots are shown in Figure 19 for a typical distorted wake and a classical wake model. The computer time required by the Prescribed Wake Program normally varies from approximately 15 seconds to 2 minutes (UNIVAC 1108 computer) depending on the number of blades, number of wake elements, and number of internal iterations required.

For all applications reported herein, the blade-wake model in the Prescribed Wake Program was represented as follows:

Number of blade segments	15
Number of wake filaments per blade	16
Number of wake revolutions	11
Wake azimuth increment	30 deg

The 15 blade segments were distributed such that 10 were spaced at 0.02 R intervals over the outer 20 percent of the blade span. Wake revolutions beyond the eleventh were found to have a negligible effect on rotor performance.

PRESCRIBED CLASSICAL WAKE ANALYSIS

The use of a classical wake in the UARL Prescribed Wake Program forms the Prescribed Classical Wake Analysis. This analysis is, in many respects, similar to the Goldstein-Lock Analysis described above, in that a finite number of blades is assumed, each blade is represented by a lifting line, and an undistorted wake geometry is prescribed. The primary differences in the analyses are as follows:

1. The helical sheets of vorticity representing the blade wakes are approximated by a finite number of discrete trailing vortex filaments to facilitate numerical solution (on a computer) of

basically the same equations which, for the optimum case, Goldstein solved analytically. The availability of a numerical solution also permits a more direct solution of the inverse problem wherein the geometry of the rotor is specified as opposed to the circulation distribution.

2. The wake geometry assumed in this version of the analysis differs from that for the Goldstein optimum wake in that the axial transport velocity of each vortex element in the wake is constant with radius and is equal to the momentum value. Tangential transport velocities are assumed to be zero. For the low helical wake pitch angles associated with helicopter rotor disc loadings, the outer portion of the wake used approximates the Goldstein wake.

A sample plot of the classical wake trajectory was presented in Figure 19.

PRESCRIBED DISTORTED WAKE ANALYSIS

This analysis differs from the previous analysis in that a more realistic, generalized distorted wake geometry based on experimental flow visualization data is used as input to the Prescribed Wake Program. Rather than input coordinates for each vortex element in the wake, equations (1) through (5) given in Reference 1 are used to define the wake and the individual coordinates are computed in the program. Use of the wake equations greatly simplifies the input requirements while retaining sufficient accuracy for the computation of induced velocities at the rotor blades.

Figure 19 indicates how the computer transforms the input wake constants to coordinate form and plots the resulting wake pattern. On the left side of this figure are the top and side views of the computer representation of a typical distorted wake. For clarity, only the wakes from 1 blade and 12 vortex filaments are shown. For this test condition, 5 of the 16 vortex filaments over the outer 8 percent of the blade were used to represent the tip vortex. The spanwise division between the vortex sheet and tip vortex regions is determined by the requirement that the vortex filaments grouped in the tip vortex have the same circulation sense and one which is consistent with a negative derivative of the final computed bound circulation distribution ($-d\Gamma/d\bar{r}$) over the tip region of the blade. This results in the radial location of the peak bound circulation as the dividing point between the inboard sheet and tip vortex portions of the wake. An iteration is built into the computer program to

insure this consistency. The roll-up of the tip vortex filaments into a single filament was approximated by truncating the inner tip vortex filaments at an input azimuth (30 degrees was used in this investigation) and assigning the experimental tip vortex geometry and the combined circulation strength to the remaining filament (Figure 19). In addition, the inboard vortex sheet which had not rolled up with the tip vortex was allowed to extend for as many revolutions as the tip vortex.

EVALUATION OF THEORETICAL METHODS

MODEL BLADE AIRFOIL DATA

Airfoil data in the Reynolds number-Mach number ranges of the model rotors are extremely limited. Therefore, the airfoil data used in the theoretical calculations were based on extrapolations of available two-dimensional data, together with adjustments made through a synthesization procedure, to provide correlation between the test results for the two-bladed rotors and the results of the Goldstein-Lock Analysis. Initial airfoil data were estimated from data given in Reference 2 for the NACA 23112 airfoil and in References 8 through 10 for the NACA 0012 airfoil. Performance results were first compared on C_T/σ versus C_Q/σ plots for the three tip Mach numbers tested to determine the general quality of correlation between test and the Goldstein-Lock Analysis. More detailed comparisons were then made on C_T/σ versus θ_{75} and C_Q/σ versus θ_{75} plots to estimate the relative magnitude of change required in the airfoil lift-curve slope and drag data to improve correlation. Approximately five iterations were required at each tip Mach number condition to achieve acceptable correlation in both the thrust-torque results and the thrust-torque-collective pitch results. The final synthesized airfoil data based on two blades (Figures 20 and 21) were then used in all other theoretical calculations. The use of synthesized airfoil data based on two blades is consistent with the procedures of Reference 1.

The airfoil characteristics above 8 degrees shown on Figures 20 and 21 could not be synthesized accurately since the rotors were not tested in a fully stalled condition (at least according to the theory used in the synthesizing process). The stall characteristics for the NACA 0012 and the NACA 23112 were estimated from available low-Reynolds number (500,000) data.

It should be noted that at the same nominal flight condition, the distorted wake analyses produce section angles of attack well above those from the Blade Element Momentum and Goldstein-Lock Analyses.

EVALUATION OF PERFORMANCE METHODS

The performance prediction methods were evaluated by comparing the results with experimental data for two model rotors and one full-scale rotor. The two model rotors were 6-bladed configurations, and the full-scale rotor was a Sikorsky six-bladed 72-foot rotor which was tested on the large-scale whirl tower. The blade chord for the full-scale rotor

was approximately 2.4 feet with a Sikorsky designed cambered airfoil section having two-dimensional lift characteristics similar to the NACA 23112 airfoil. The results are discussed below.

Model Rotors

Performance Predicted for Rotors With Cambered Blades

The performance results from the Blade Element Momentum, Goldstein-Lock, Prescribed Classical Wake, and Prescribed Distorted Wake Analyses are presented in Figure 22 for a 6-bladed rotor with an NACA 23112 airfoil section operating at 600 feet/second tip speed. The results from each method are compared on a C_T/σ versus C_Q/σ plot with symbols indicating the theoretical points calculated at nominal values of collective pitch. The test data from Figure 9b are presented again in Figure 22 for comparison with corresponding theoretical data. The performance predicted by the Blade Element-Momentum and Goldstein-Lock methods correlated well with the experimental C_T/σ and C_Q/σ at low thrust levels (below C_T/σ of 0.07); however, the performance becomes increasingly optimistic with increasing thrust for both methods. The Prescribed Classical Wake method did not demonstrate a similar trend with increasing thrust. In fact, excellent correlation appears to have been achieved up to 12 degrees collective pitch. This apparent correlation at high collective pitch values (10 through 12 degrees) is misleading since it was established in Reference 1 that the Goldstein-Lock and Prescribed Classical Wake Analyses, because of improper wake simulation, are not reliable for predicting performance for 6-bladed rotors at high thrust levels. The correlation of the classical wake results in Figure 22 can be related to the use of synthesized airfoil data and the method used to generate these data. Since a 2-bladed rotor and undistorted wake analysis were used (Goldstein-Lock), possible offsetting effects due to the synthesized data and undistorted wake, particularly in the stall region, could produce small performance differences sufficient to indicate correlation with the test results.

The distorted wake performance curve shown in Figure 22 was generated using a wake geometry based on the generalized wake procedure of Reference 1. As indicated in that reference, the performance is very sensitive to the tip vortex axial position, particularly at the higher thrust levels as shown in Figure 22. At the 11 degree collective pitch condition shown in Figure 22, the distorted wake results indicated a thrust level approximately 6 percent greater than the experimental level at the same power. This could be the result of inaccuracies of the

synthesized airfoil data at high angles of attack and/or from inaccuracies in the wake geometry used. For example, a 0.01 R upward displacement of the tip vortices as they passed beneath the following blades produced correlation. Adjustments in the tip vortex position by 1 percent of the radius are not unreasonable since the accuracy of the measurement of this position was approximately 1 percent. The cambered blades permitted operation of the rotor at thrust levels considerably in excess of those encompassed by the charts of Reference 1. Without a complete set of model two-dimensional airfoil data, it is not possible to identify the exact cause of the discrepancy. For full-scale blades, where airfoil data and wake data are available, any such discrepancies would be amenable to analysis.

Section Characteristics of Cambered Blades

The difference in the performance results of the various analytical methods became more explicit when comparing the individual blade aerodynamic characteristics. Figure 23a presents the radial distributions of axial induced velocity and section angle of attack predicted by the four methods. Shown also on Figure 23a are the tip vortex and inboard sheet positions of the wake used in the Prescribed Distorted Wake Analysis. The most significant difference noted in these distributions is the induced velocity and angle of attack near the blade tip for the distorted wake case. It is evident from the position of the tip vortex from the preceding blade that a significant upward velocity will be induced outboard of this point and a downward velocity inboard. As shown in Figure 23a, the downward velocity results in an angle of attack approximately equivalent to the nondistorted wake methods; however, outboard of the vortex the induced angles of attack reach levels nearly twice as great. The effects of the wake-distortion on the blade thrust and torque distributions are shown in Figure 23b; they indicate that the improved performance shown in Figure 22 results largely from an increase in lift near the blade tip. Although the section characteristics with the vortex located nearer the blade are not shown, the effect of moving the vortex was to reduce the angles of attack inboard, thereby reducing the lift, and to increase the angles outboard, producing incipient stall without an increase in lift. A slight reduction in torque occurred inboard; however, a significant increase was produced outboard due to stall. Therefore, it is imperative to accurately define the wake geometry, especially the tip vortex position, when predicting rotor hover performance.

Performance Predicted for Rotors With Tapered Blades

The performance for the 6-bladed rotor with 2:1 planform taper is shown in Figure 24 for a tip speed of 600 feet/second. The predicted performance agrees with the test results at lower thrust levels, but becomes excessively optimistic with increasing thrust. The discrepancies between the test and theoretical results are considerably more prominent for the tapered blades than for the cambered blades. The discrepancies appear to be related primarily to vortex-induced blade stall and the lack of systematic wake geometry data for rotors having tapered blades. Due to the limited scope of this investigation, the condition shown in Figure 7b for the 6-bladed rotor operating at 600 feet/second tip speed and 6.7 degrees collective pitch is the only tapered blade configuration for which flow visualization data were obtained. Therefore, the following conclusion for the tapered blade wake must be considered within the limitation of the flow visualization data. It was seen in the flow visualization pictures of Figure 7 that the blade tip vortex of the tapered blade moved downward at a slower rate than did the vortex for the cambered blade. In fact, the movement of the vortex was delayed sufficiently to cause impingement of the vortex on the following blade. The Prescribed Wake Analysis is not currently equipped to accept blade-vortex intersections since data are not available to define the velocity distributions within the vortex core and the behavior of a vortex filament when it impinges on a rigid body such as a blade. The only wake geometry data available for this investigation was that obtained from Reference 1 for constant-chord, linearly twisted blades. Apparently, such data are not applicable for tapered blades. The limited photographs taken during this study (Figure 7) were not sufficient to develop a generalized wake for tapered blades. As a result, the constant-chord, zero-twist data of Reference 1 were used to generate the distorted wake performance curve of Figure 24. For completeness, this curve has been included; however, it should be noted that significantly improved performance prediction would be expected if accurate tapered-blade, wake geometry data were used.

Since it is evident that proper tip vortex representation is vital to accurately predict tapered blade performance, it is not surprising that the methods assuming no wake distortion are also inadequate to predict tapered blade performance. This is borne out in the poor agreement with the test results shown in Figure 24. It becomes obvious that additional wake geometry investigations must be conducted before a reliable tapered blade performance method is available. This should also be coupled with a test program to define model airfoil two-dimensional characteristics as a function of Mach number. Since adequate tapered

blade wake geometry data were not taken (recording of such data was beyond the scope of this investigation), reliable blade section characteristics could not be computed; however, the general trends would be expected to be similar to the cambered blade results presented in Figure 23.

Full-Scale Rotor

The theoretical methods described previously were also used to calculate the hover performance of a full-scale 6-bladed rotor with blades having a cambered airfoil developed and tested by the Sikorsky Division of UAC. Sectional lift and drag data for the airfoil were supplied by Sikorsky, and the data were applied to all the full-scale performance calculations. The results of the theoretical calculations are shown in Figure 25 and are compared to the experimental data, which have been corrected for ground and hover-stand interference effects. As shown in Figure 25, the performance is optimistic for the results predicted by the Blade Element-Momentum, Goldstein-Lock, and Prescribed Classical Wake methods (all undistorted wake analyses). Although only one hovering condition was investigated, these results are consistent with other full-scale theoretical results presented in Reference 1 for these same performance methods. The performance was also predicted with the Prescribed Distorted Wake method, where the wake geometry was based upon the generalized wake procedure of Reference 1. The results of Figure 25 show that the prescribed wake method with wake distortions produced a thrust level slightly below the test results; however, correlation can be improved with minor adjustments in the tip vortex axial position within the accuracy of the wake data. For example, by positioning the tip vortex 0.005 R farther below the rotor disc, the performance represented by the semicircular point in Figure 25 is obtained.

The spanwise distributions of induced velocity and section angle of attack are shown in Figure 26 for the 12.9-degree collective pitch condition shown in Figure 25. The prescribed distorted wake results indicate a rapid increase in angle of attack near the tip, which has been caused by the strong influence of the distorted tip vortex on the induced velocity distribution. This characteristic increase in angle of attack near the tip of the blade has been substantiated by tests on the Sikorsky whirl stand, where pressure measurements were recorded at three spanwise stations over the outboard 15 percent of the blade. The angle of attack distribution and rotor performance could be calculated to within the experimental limits of the test data with the Prescribed Distorted Wake method by making small adjustments in the generalized wake of Reference 1.

This emphasizes the importance of simulating wake contraction in predicting blade section characteristics. Although this ability to calculate the details of the blade characteristics and rotor performance is encouraging, it would be desirable to substantiate the method with more comprehensive pressure data taken over the whole blade. Furthermore, a systematic investigation of the sensitivity of performance and section characteristics to small changes in the tip vortex position should be conducted, since they (performance and section characteristics) have been shown to be strongly dependent upon the tip vortex position. Thus, through these systematic variations, it may be possible to establish a procedure to adjust the generalized wake model so that it is possible to consistently predict the rotor performance.

RESULTS AND CONCLUSIONS

The results and conclusions presented below are based on model rotor tests at relatively low Reynolds numbers; however, the performance trends indicated by these results should be applicable to rotors operating at full-scale Reynolds numbers.

1. For model rotors operating at full-scale tip speeds, the use of camber significantly increases the maximum rotor lift capability relative to blades with a symmetrical (NACA 0012) airfoil section.

2. Rotors with untwisted, linearly tapered blades having a nominal taper ratio of 2:1 stall at lower thrust levels than rotors with untwisted, untapered blades. The earlier stall is related to higher blade-vortex interference caused by a reduced tip vortex vertical displacement of the tapered blade.

3. At equivalent power levels, camber increases the rotor thrust approximately 6 percent at high thrust levels, however, no improvement in performance is gained at low thrust levels.

4. Rotors with linearly tapered blades having a nominal taper ratio of 2:1 operating below stall initiation produce approximately 5 percent more thrust at a given power than a rotor without taper.

5. Camber and 2:1 blade taper do not significantly influence in-ground-effect performance.

6. Nondistorted (uncontracted) wake performance analyses generally predict higher thrust levels for cambered and tapered rotors than are measured experimentally.

7. A distorted wake performance analysis provides an improved method for predicting cambered rotor performance for model as well as full-scale rotors.

8. Tapered blade wake geometry data are needed to assess the accuracy of the distorted wake program in predicting tapered blade performance.

RECOMMENDATIONS

1. The cambered blade section used in these studies should be evaluated further. Such work should include (1) acquisition of static and dynamic airfoil characteristics at full-scale Reynolds and Mach numbers and (2) an assessment of the forward flight performance and aeroelastic characteristics.

2. Flow visualization data should be obtained for model rotors with cambered blades inasmuch as camber permits operation at thrust levels beyond those covered by existing data. Similar data should also be acquired for tapered blades.

3. Experimental two-dimensional airfoil data at the Reynolds and Mach numbers for model airfoils should be obtained to allow a more thorough evaluation of the accuracy of distorted wake analyses.

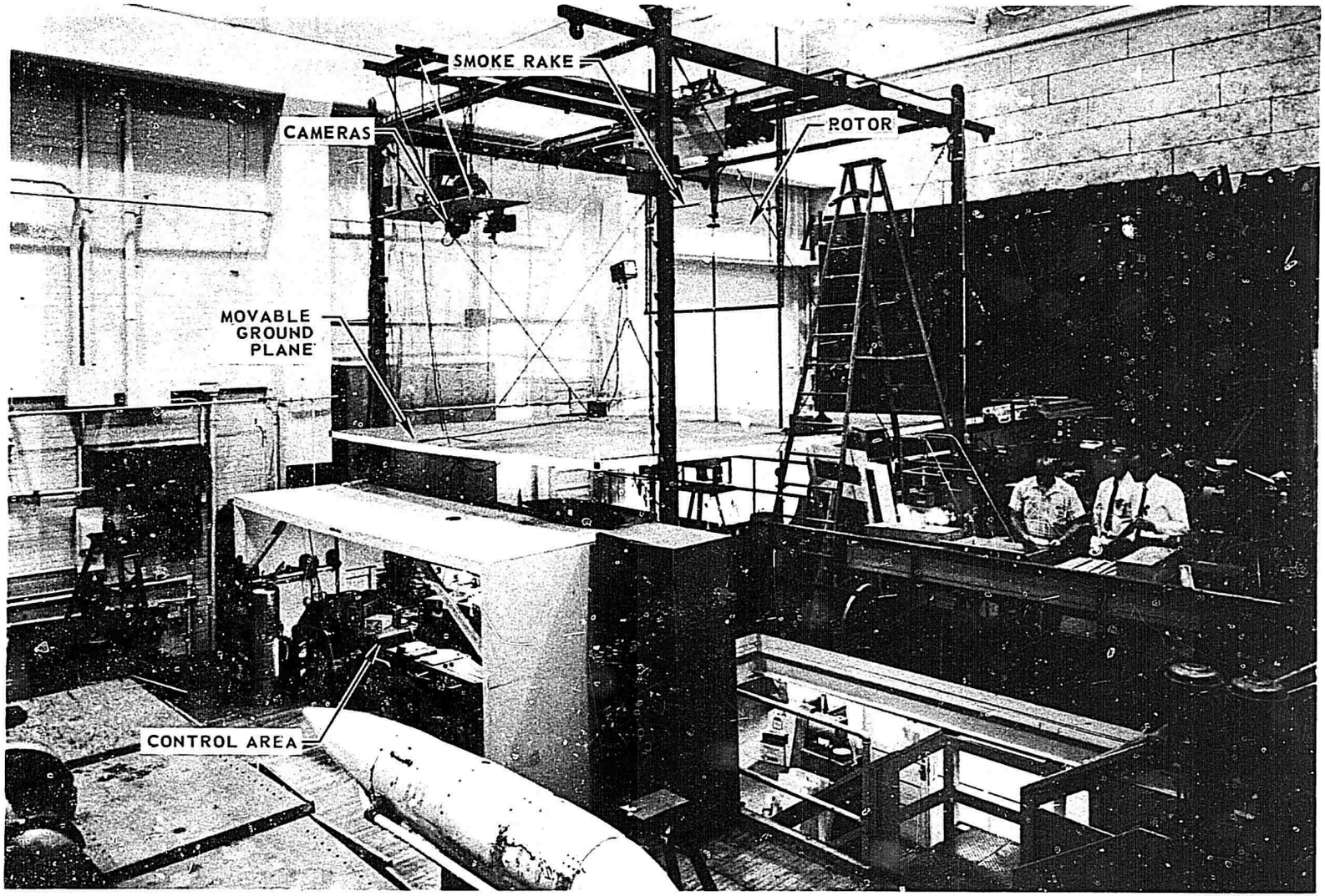

Figure 1. UARL Model Helicopter Rotor Hover Facility.

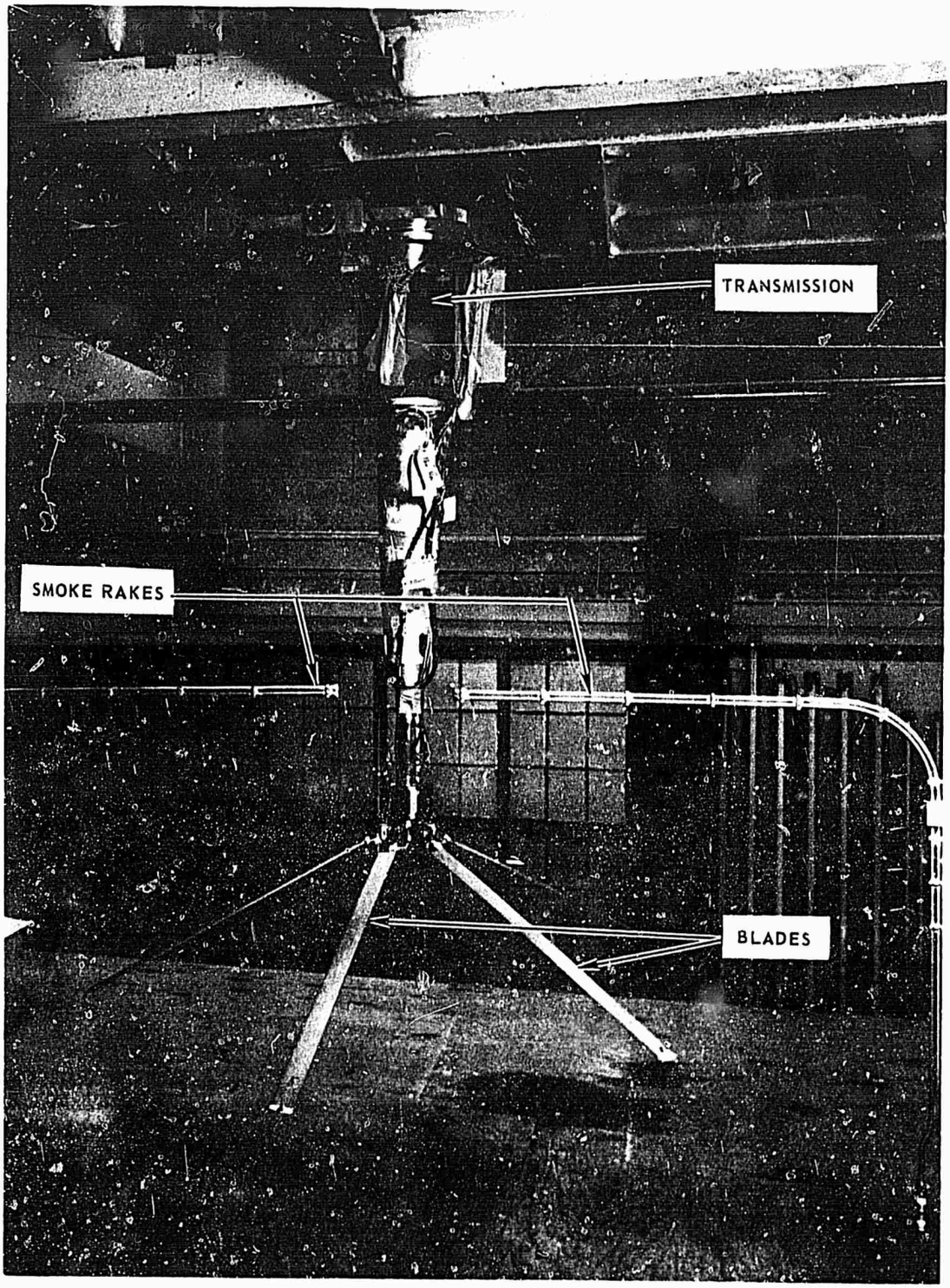

Figure 2. Rotor Test Rig.

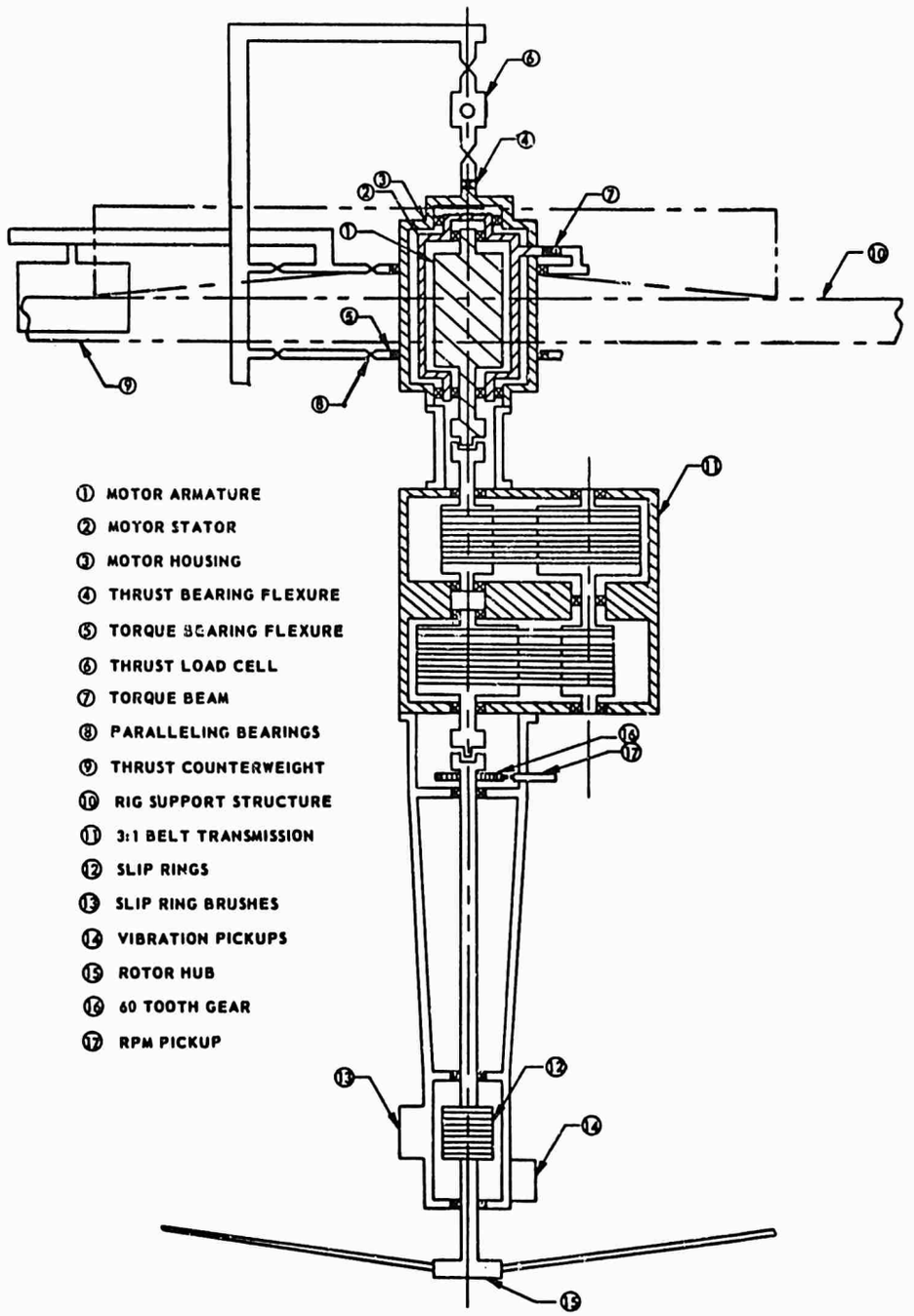

Figure 3. Schematic Cross Section of Rotor Test Rig.

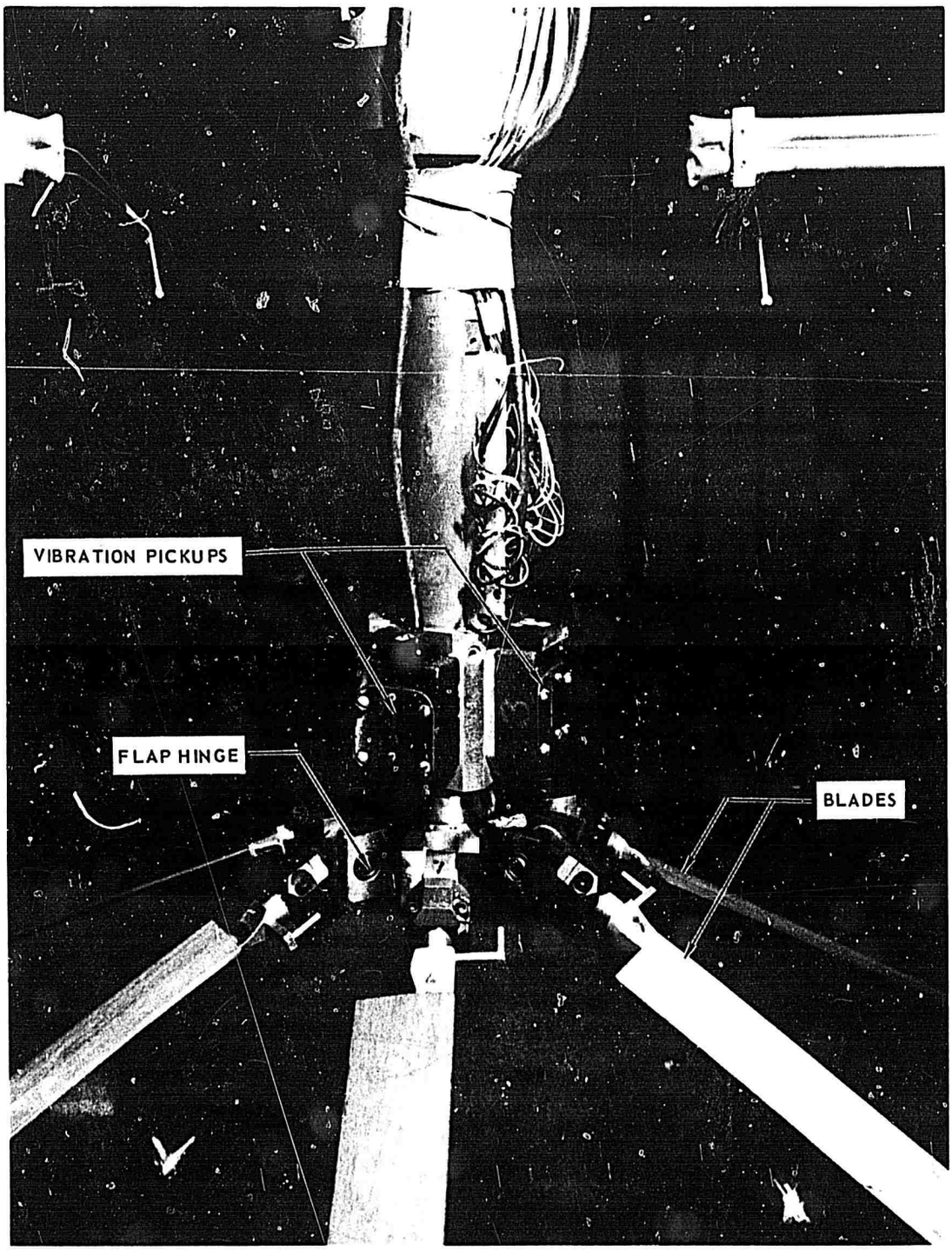

Figure 4. Rotor Hub.

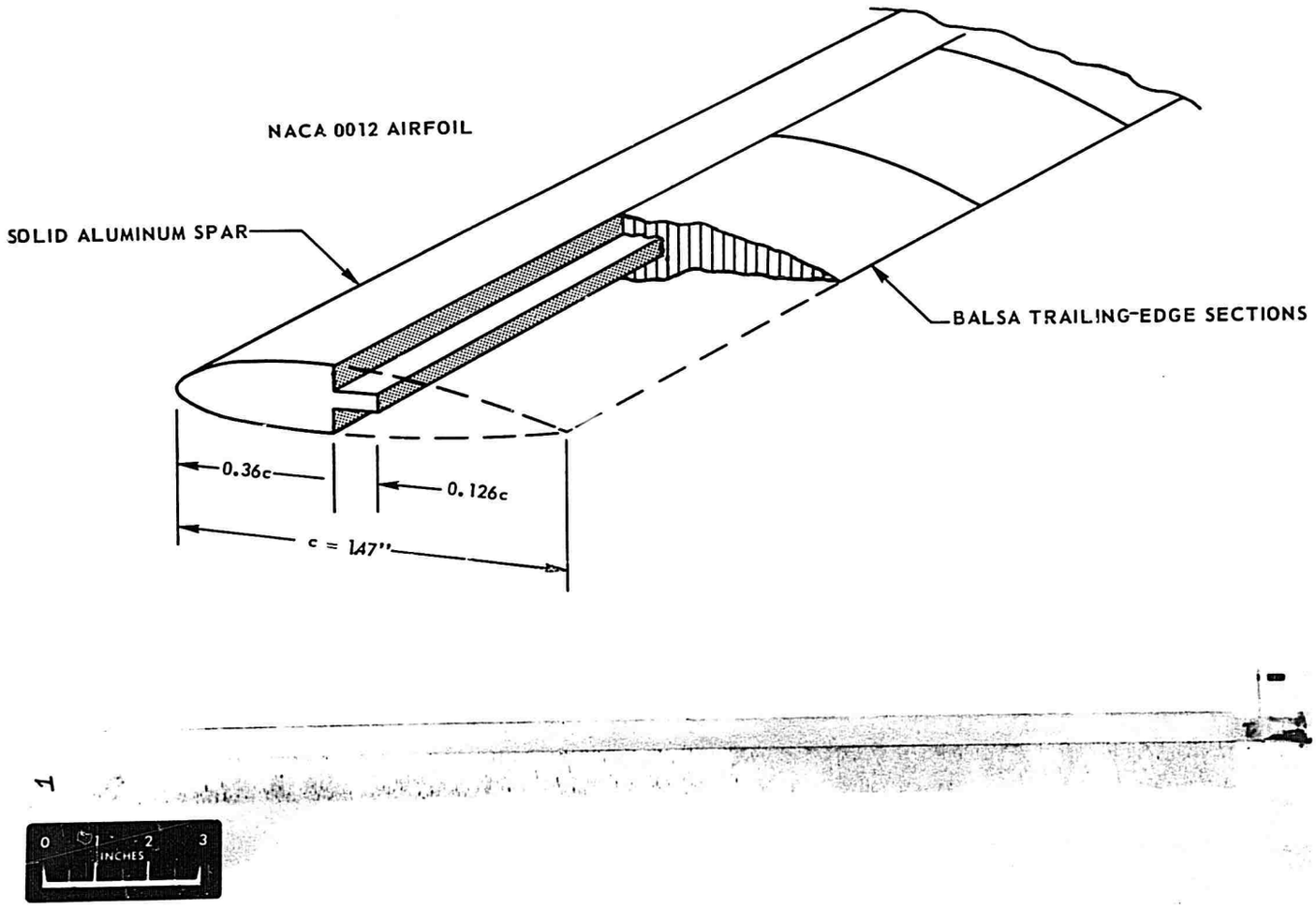

Figure 5. Schematic of Model Rotor Blade Construction.

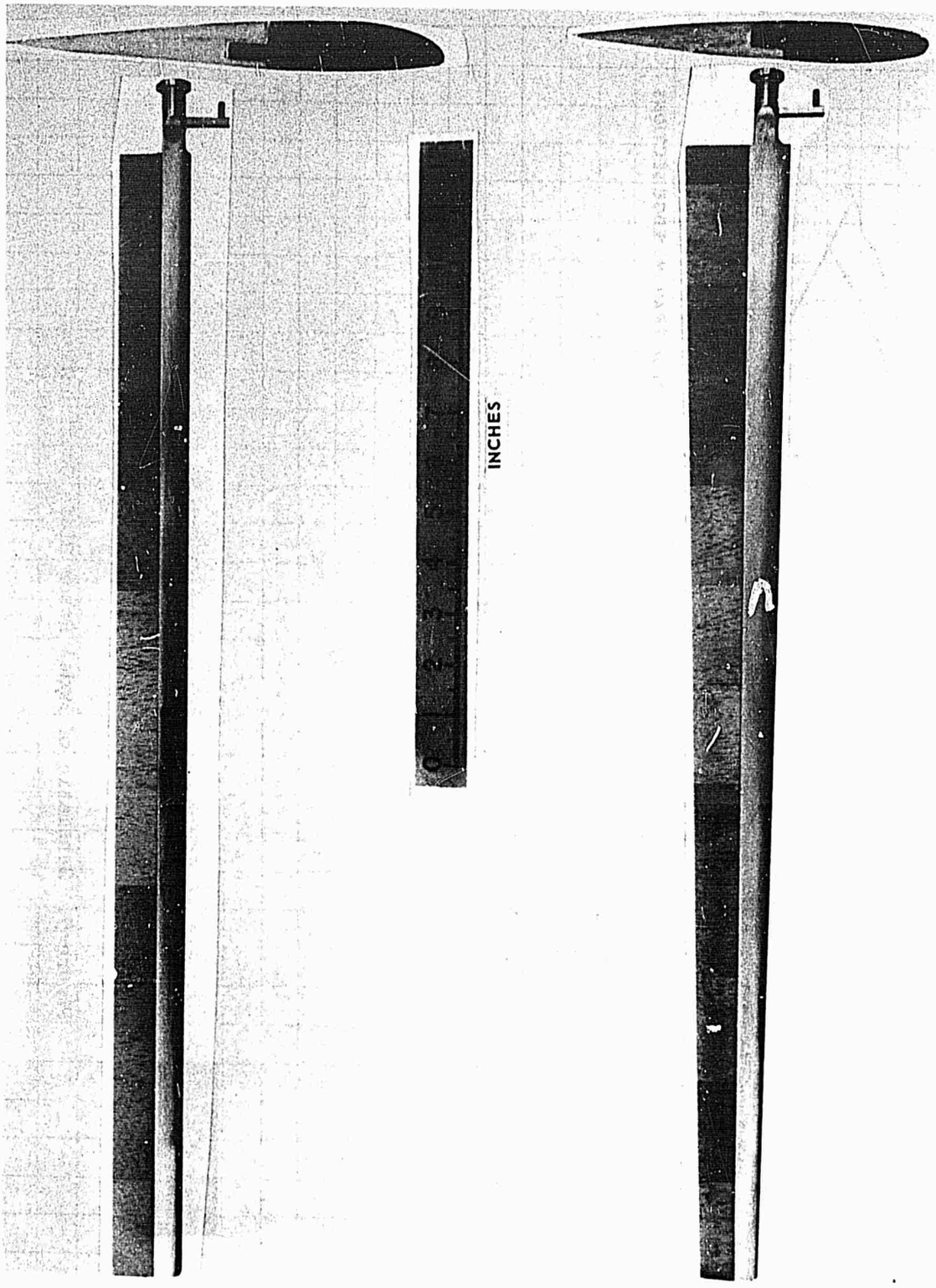

Figure 6. Cambered and Tapered Blades for Model Rotors.

$\theta_1 = 0°$ AR = 18.2 ΩR = 600 FPS $\theta_{75} = 4°$ C_T/σ = 0.0281

$\psi_w = 0°$ $\psi_w = 15°$

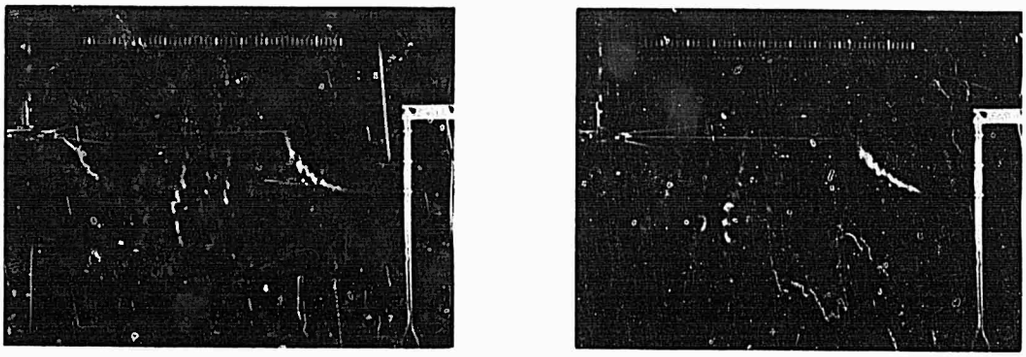

$\psi_w = 30°$ $\psi_w = 45°$

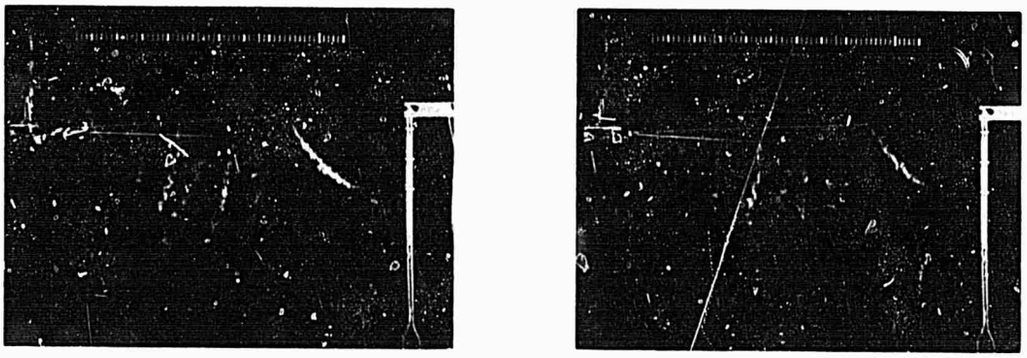

(a) CAMBERED BLADES

Figure 7. Sequence of Photographs Showing the Time History of Wake for Cambered, Tapered and Untapered Blades in Hover -- b = 6.

$\theta_1 = 0^\circ$ AR = 18.2* ΩR = 600 FPS $\theta_{75} = 6.7^\circ$ $C_T/\sigma = 0.0433$

*BASED ON THE BLADE CHORD AT 0.75R

$\psi_W = 0^\circ$

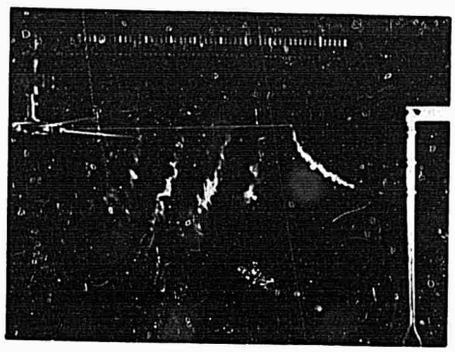

$\psi_W = 15^\circ$

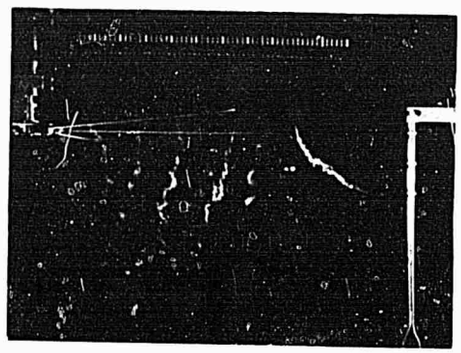

$\psi_W = 30^\circ$

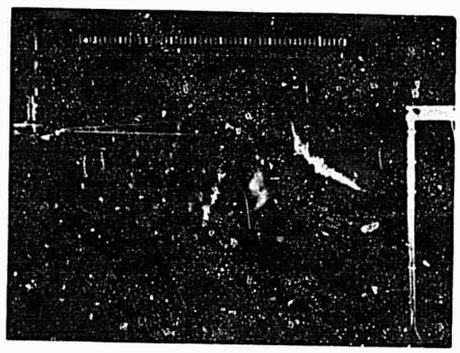

$\psi_W = 45^\circ$

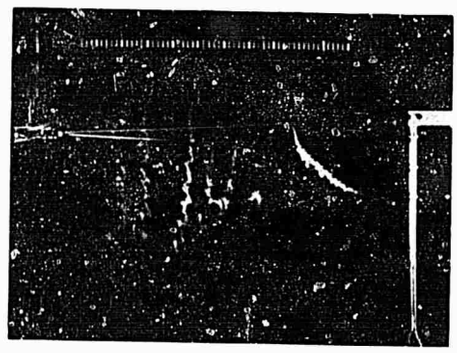

(b) TAPERED BLADES

Figure 7. Continued

$\theta_1 = 0^\circ$ AR = 18.2 ΩR = 700 FPS $\theta_{75} = 6^\circ$ $C_T/\sigma = 0.0300$

$\psi_W = 0^\circ$

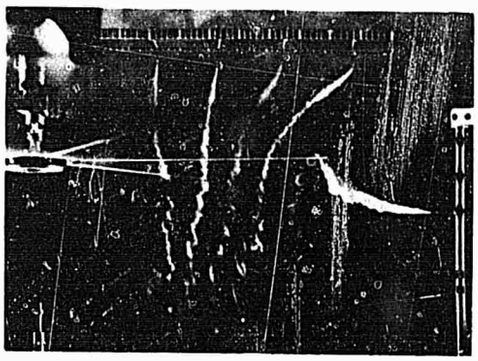

$\psi_W = 15^\circ$

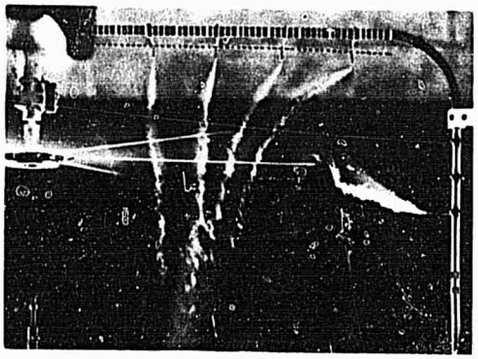

$\psi_W = 30^\circ$

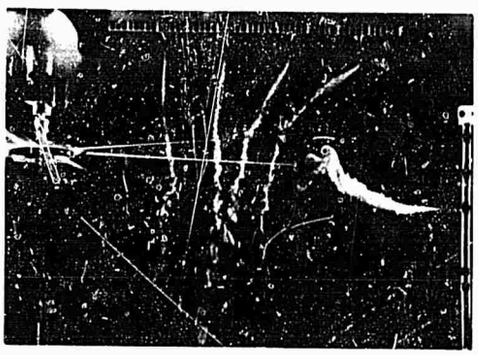

$\psi_W = 45^\circ$

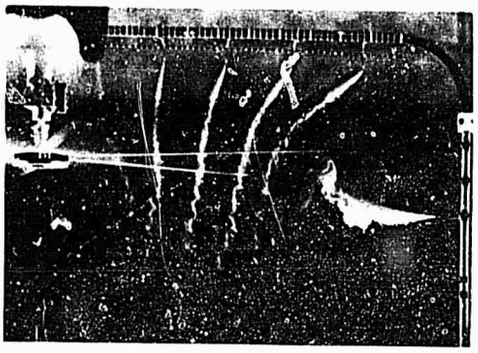

(c) UNTAPERED, SYMMETRICAL BLADES

Figure 7. Concluded.

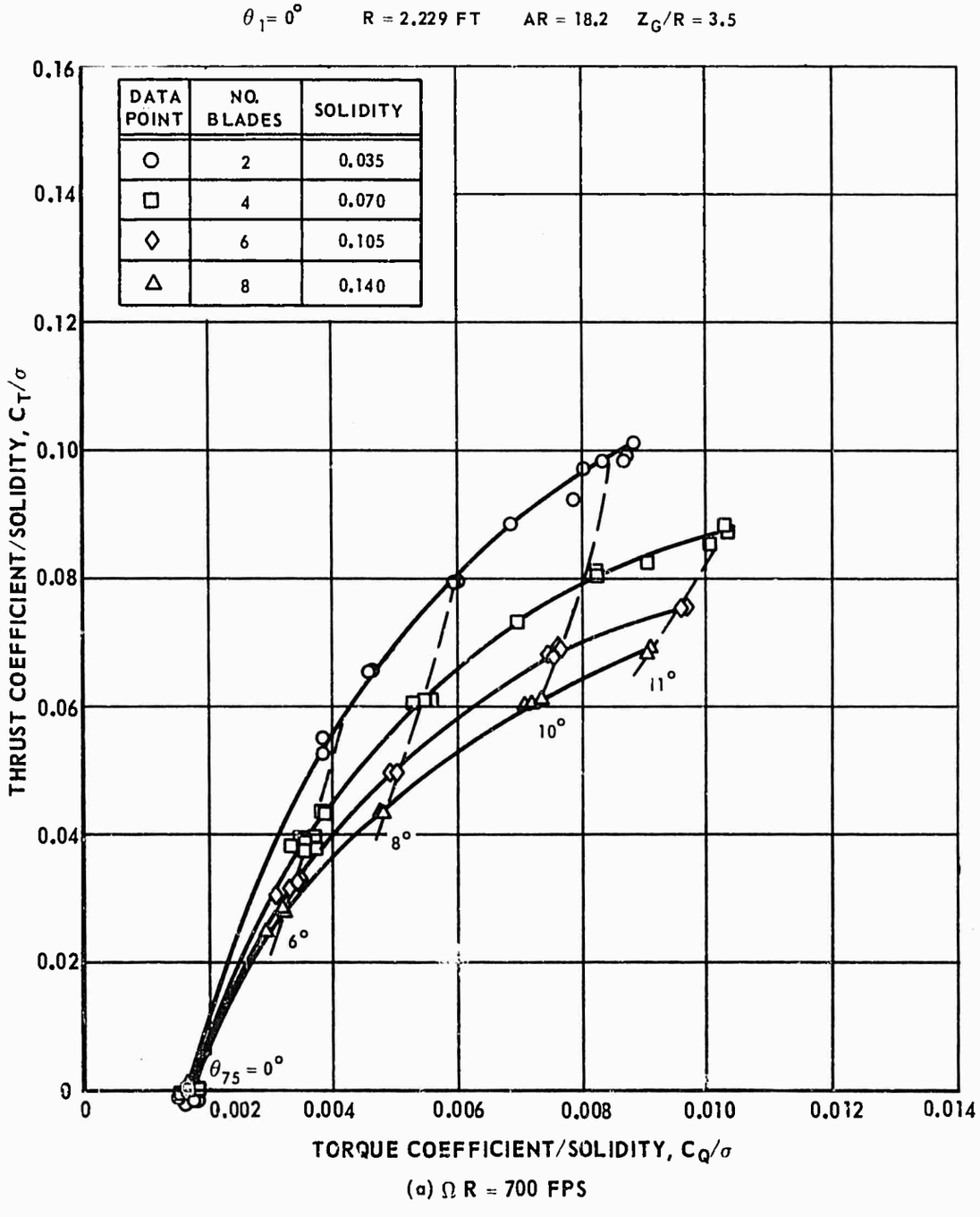

Figure 8. Experimental Model Rotor Hover Performance for Blades With NACA 0012 Airfoil Section and 1:1 Planform Taper Ratio.

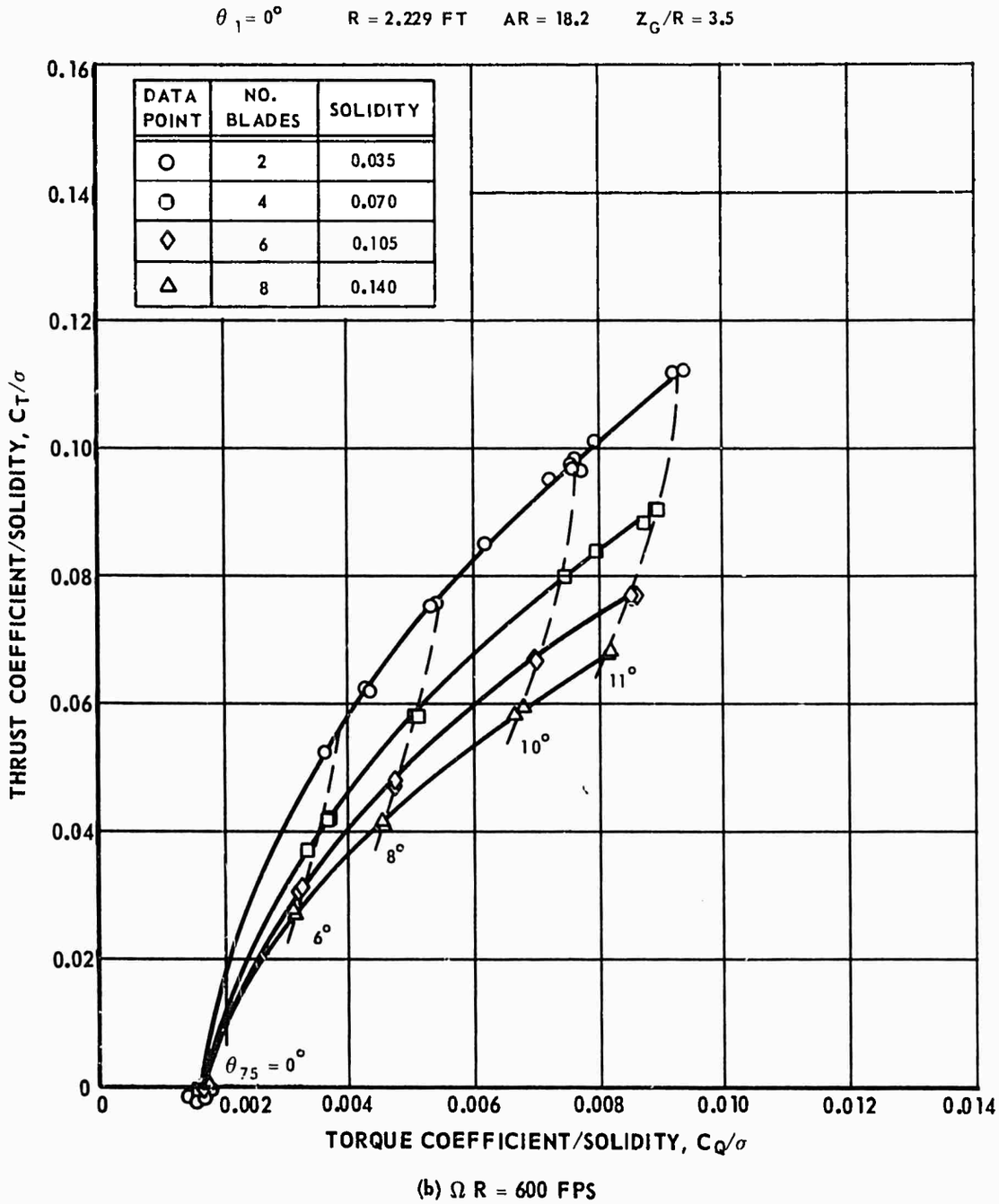

(b) ΩR = 600 FPS

Figure 8. Continued.

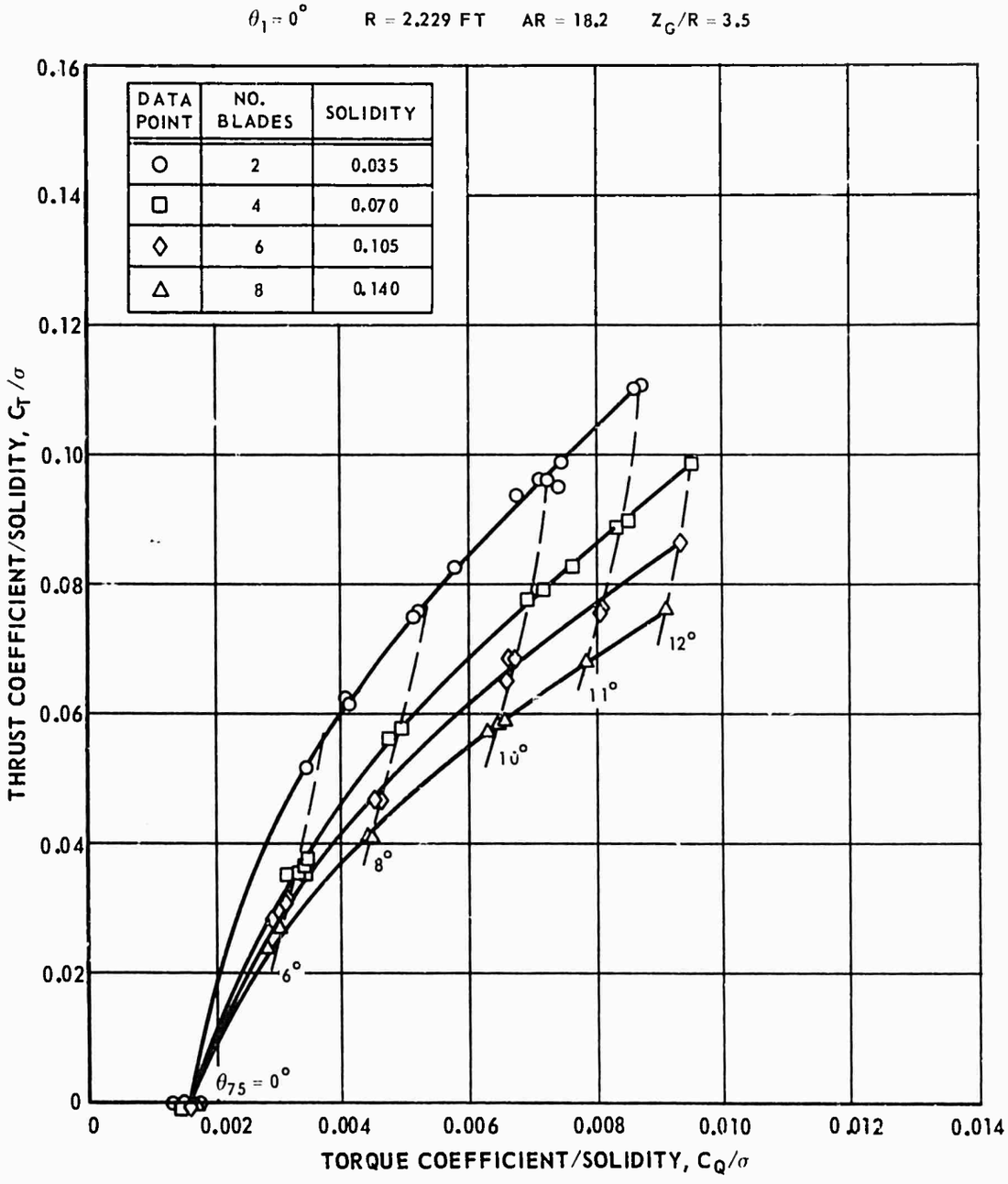

(c) Ω R = 525 FPS

Figure 8. Concluded.

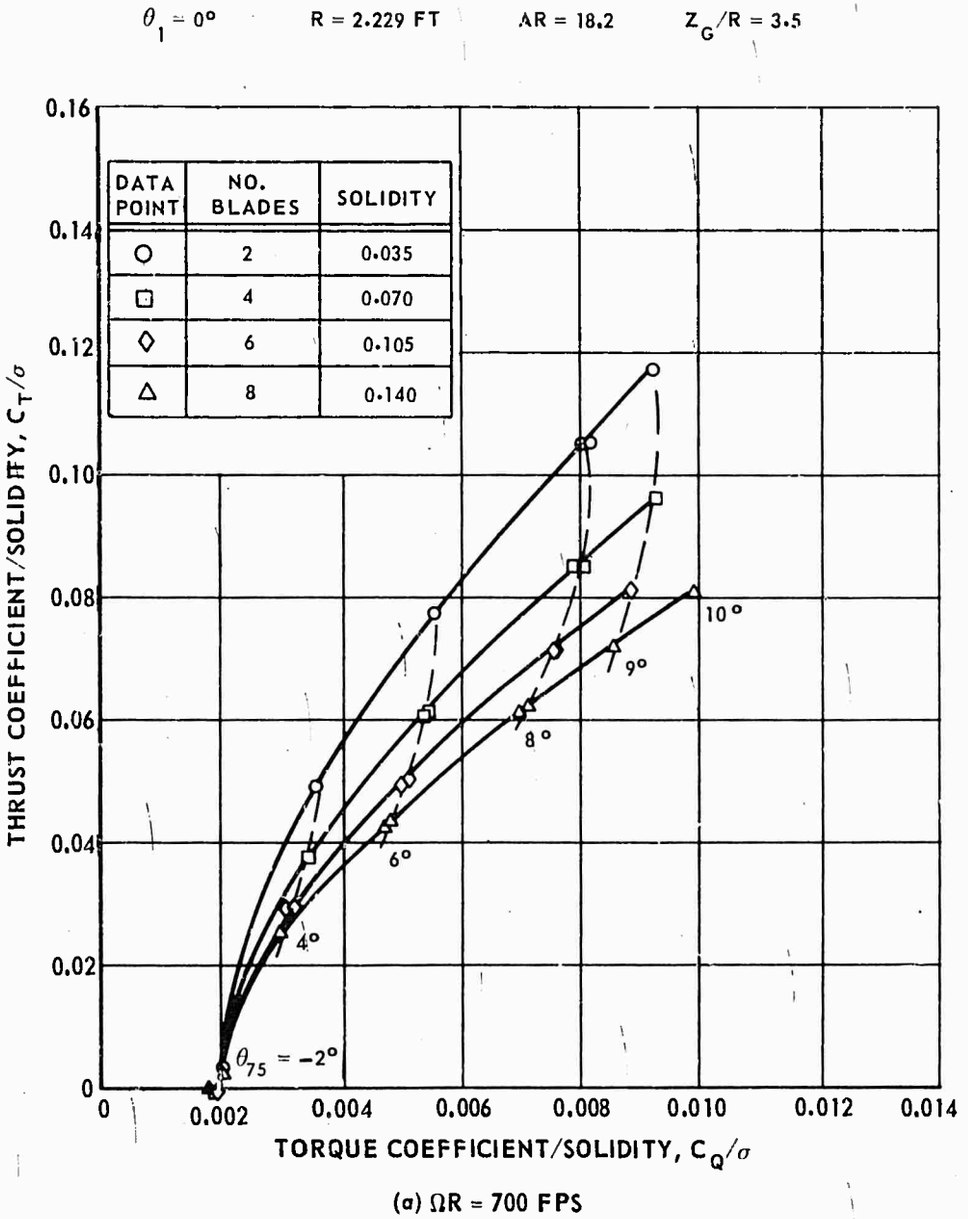

Figure 9. Experimental Model Rotor Hover Performance for Blades With NACA 23112 Airfoil Section and 1:1 Planform Taper Ratio.

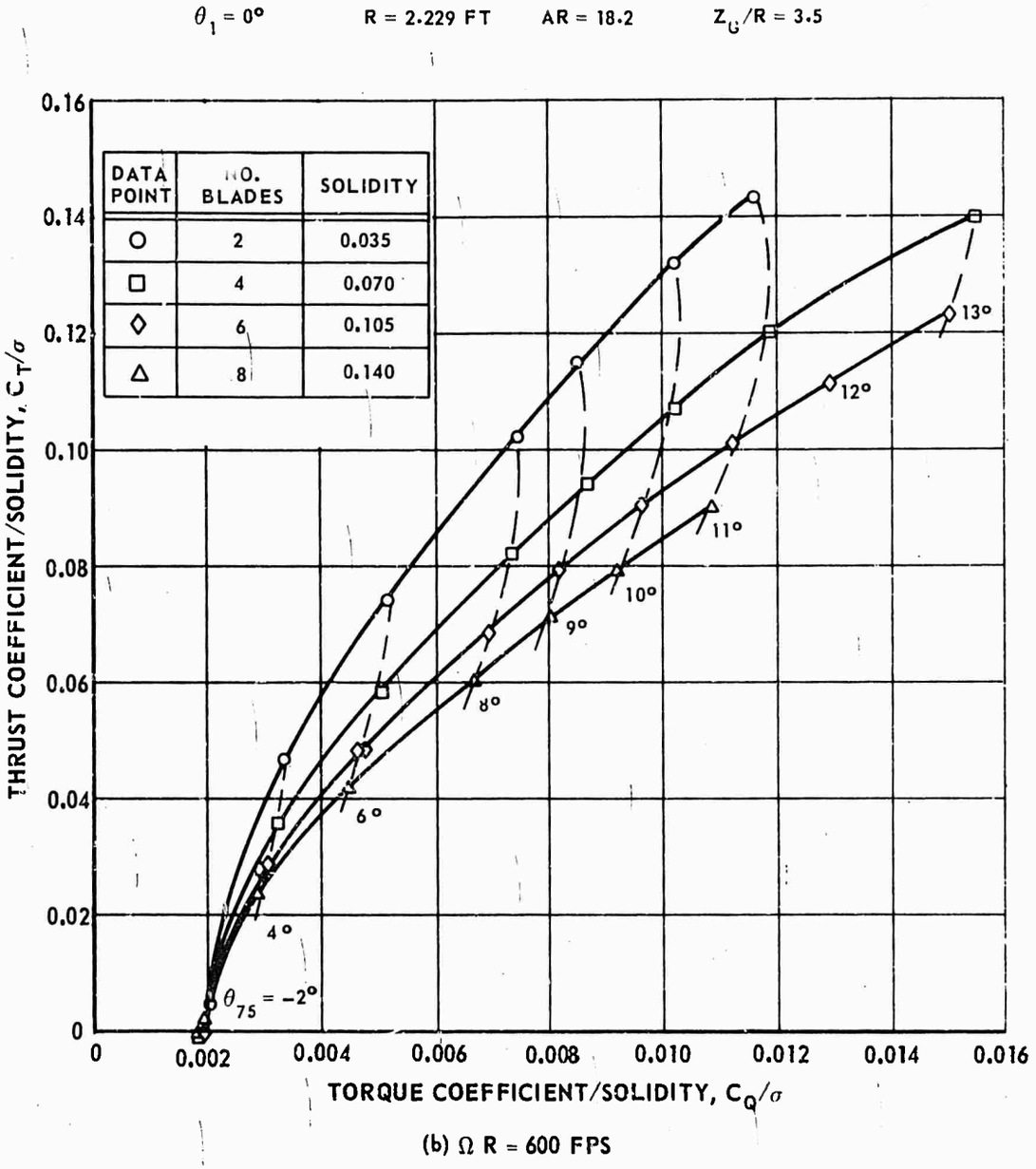

(b) Ω R = 600 FPS

Figure 9. Continued.

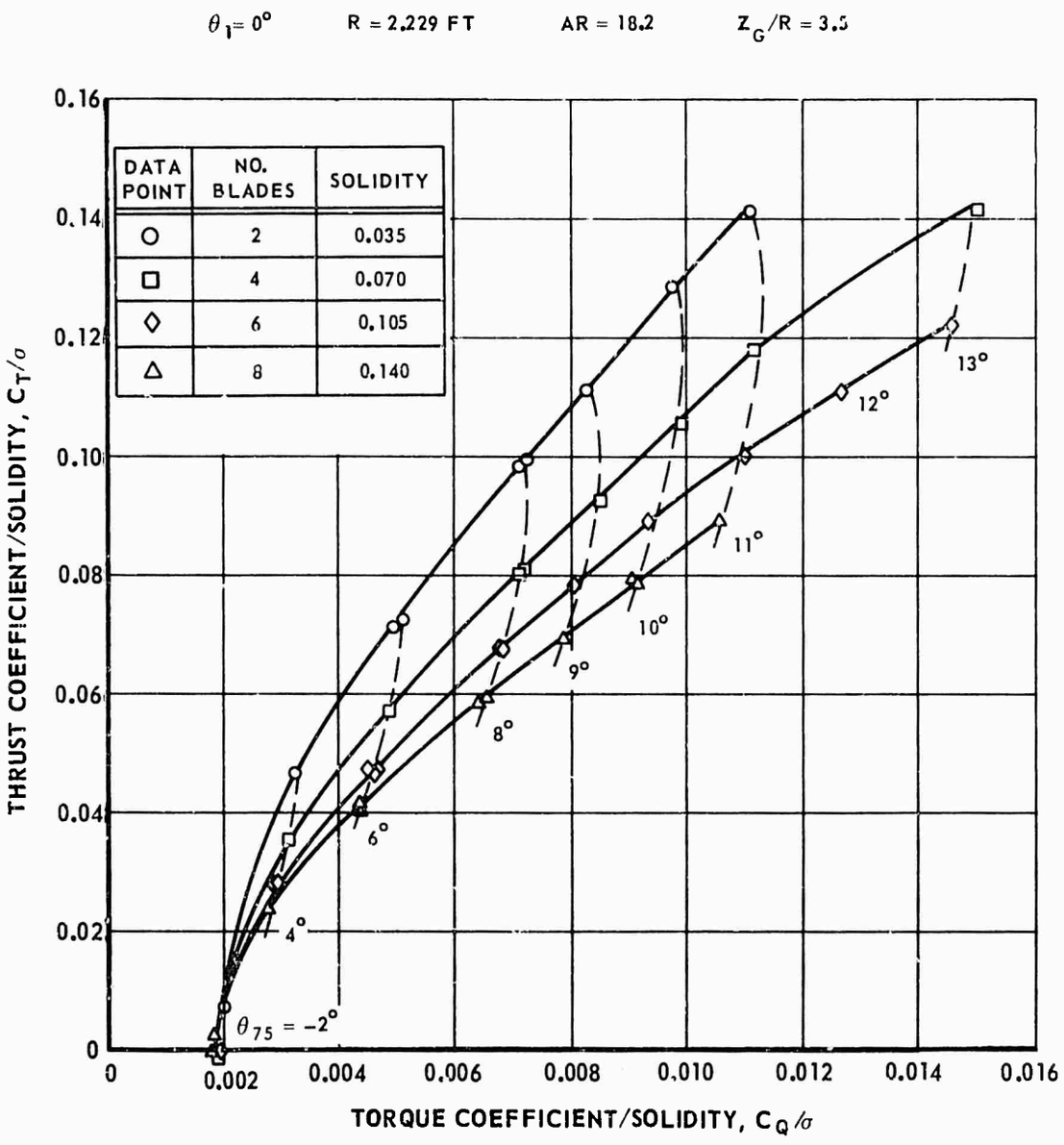

(c) ΩR = 525 FPS

Figure 9. Concluded.

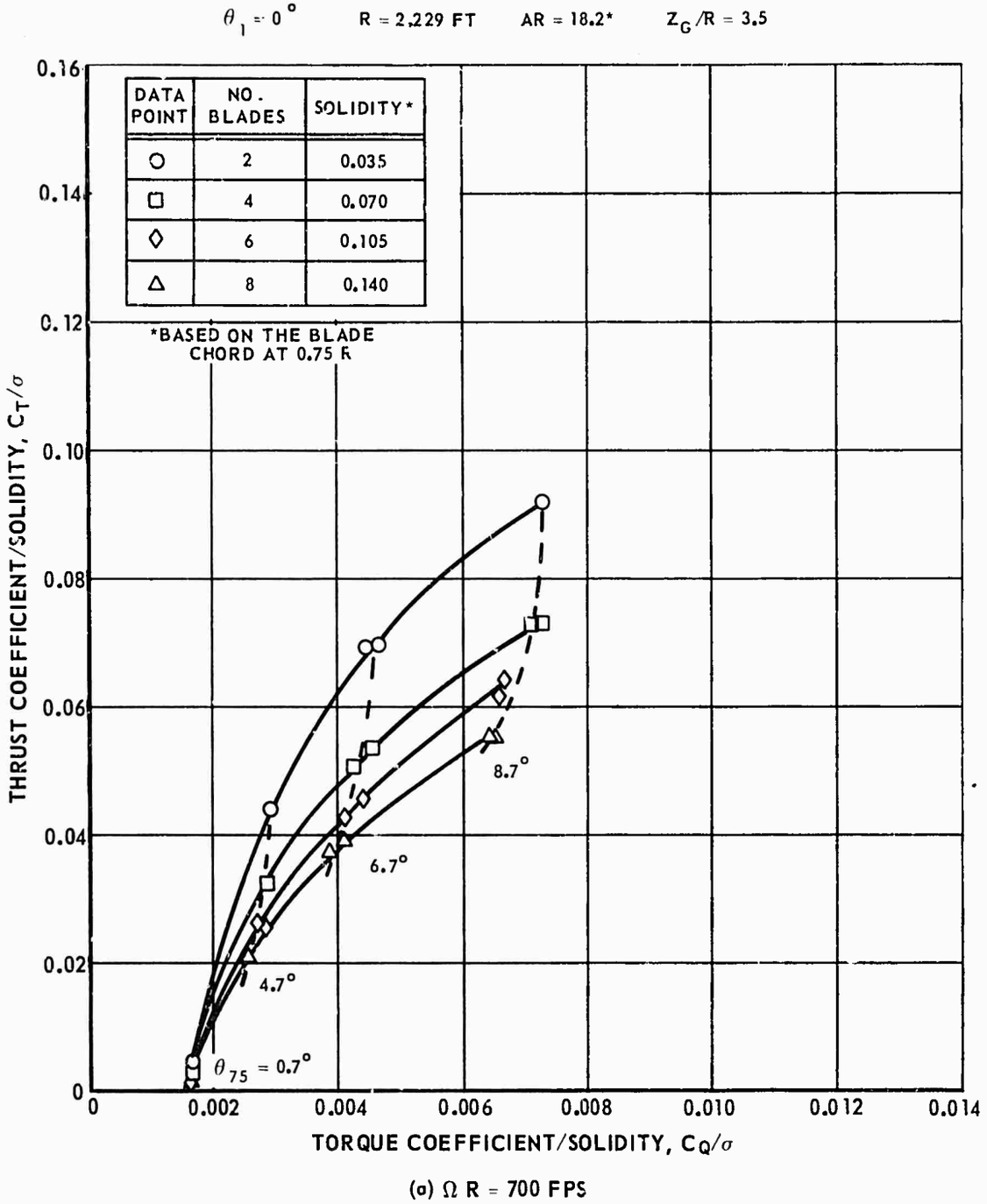

(a) $\Omega R = 700$ FPS

Figure 10. Experimental Model Rotor Hover Performance for Blades With NACA 0012 Airfoil Section and 2:1 Planform Taper Ratio.

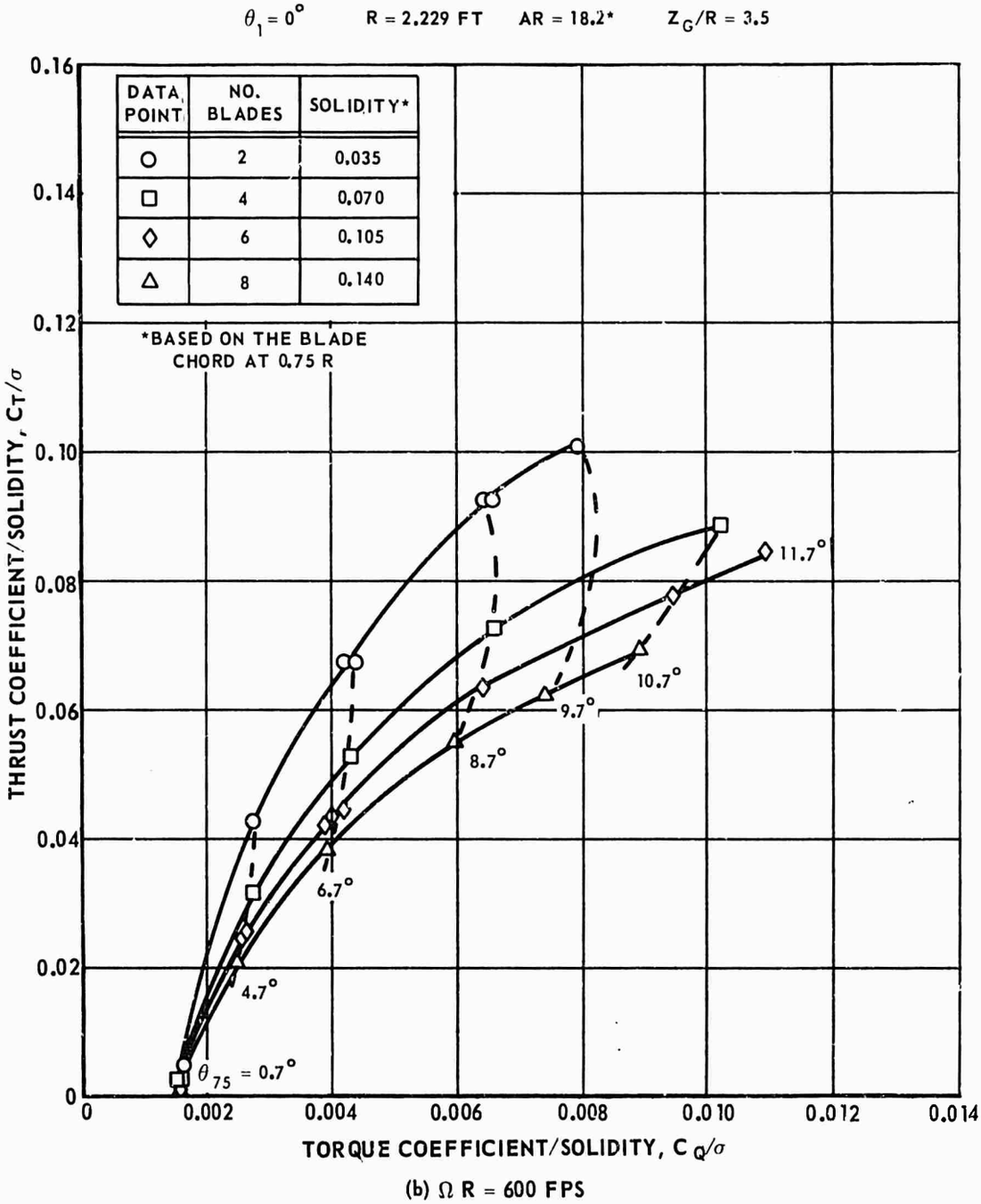

(b) Ω R = 600 FPS

Figure 10. Continued.

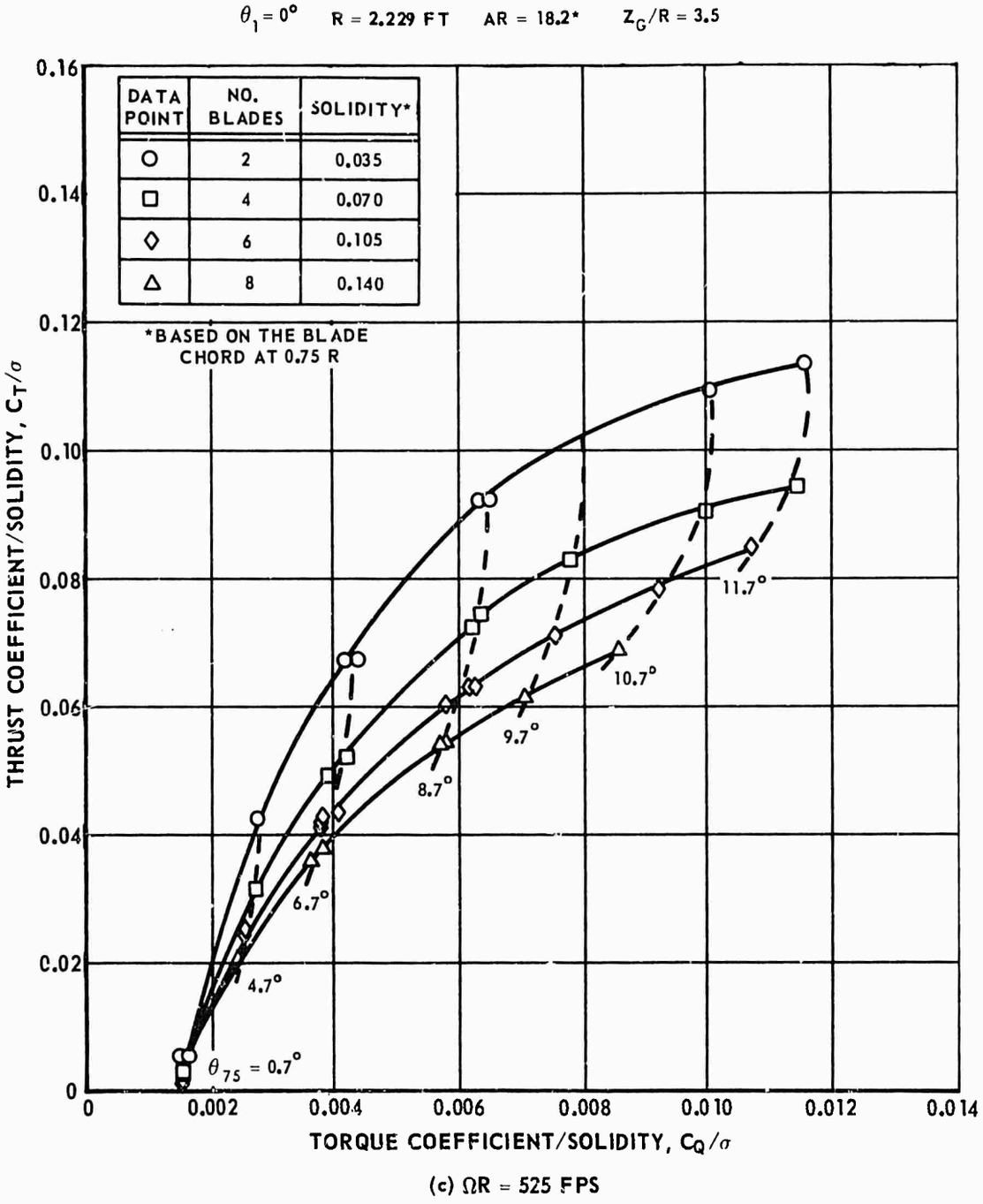

(c) ΩR = 525 FPS

Figure 10. Concluded.

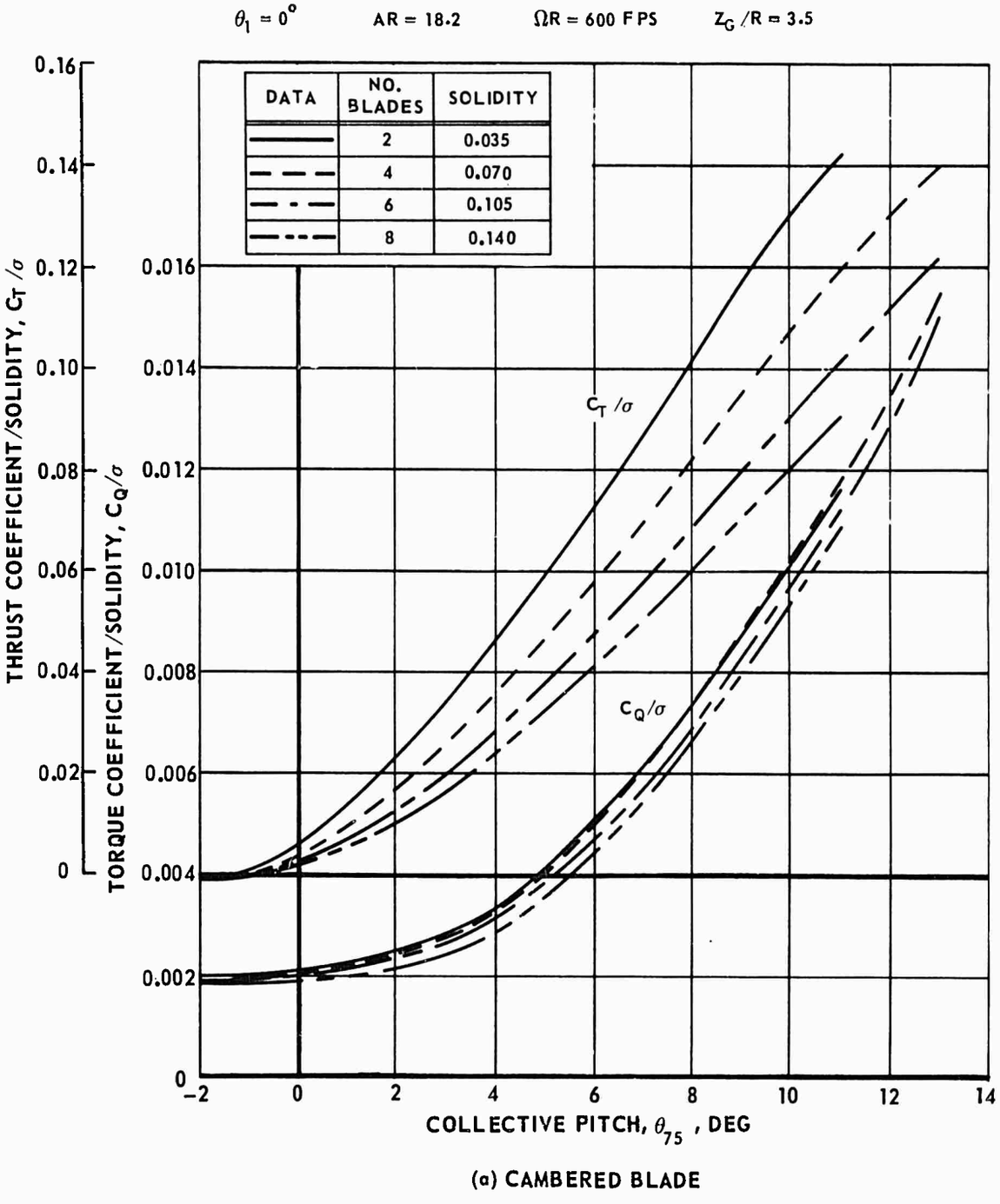

(a) CAMBERED BLADE

Figure 11. Typical Effect of Collective Pitch on Experimental Model Rotor Hover Performance.

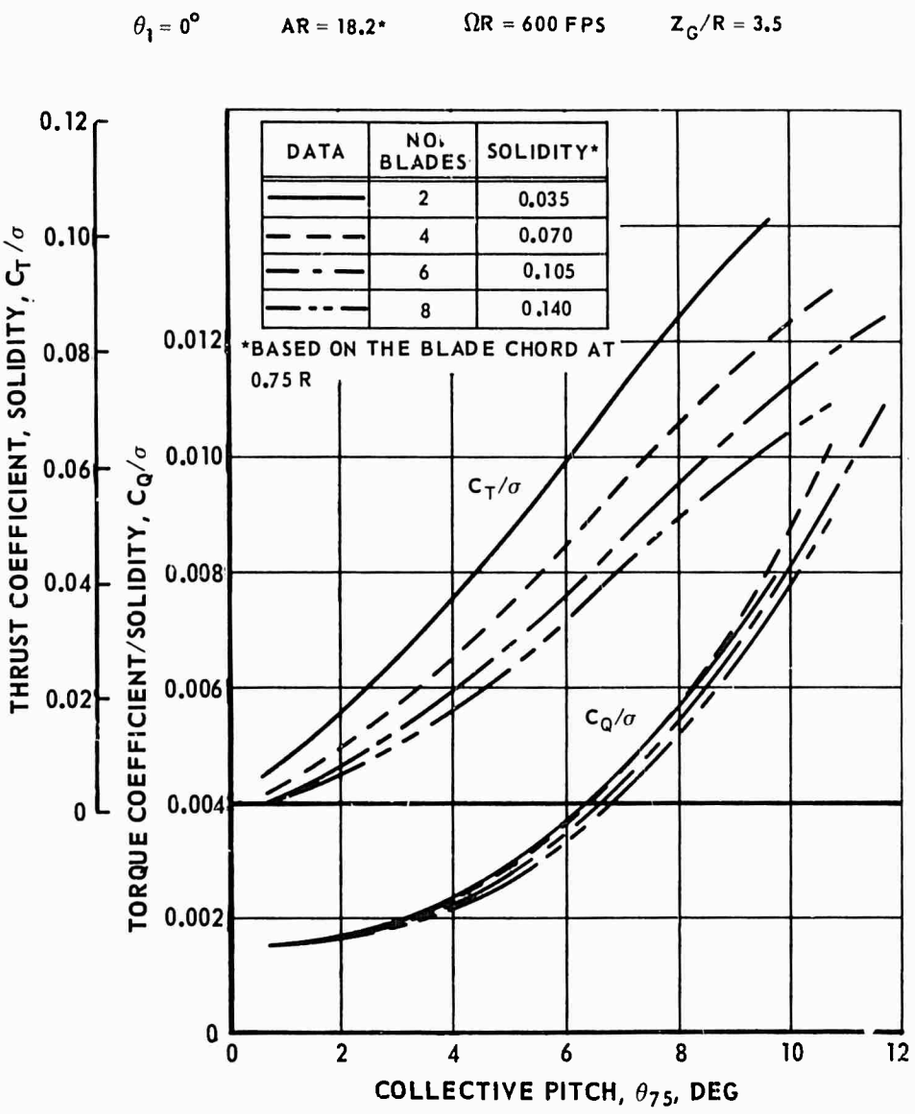

(b) TAPERED BLADES

Figure 11. Concluded.

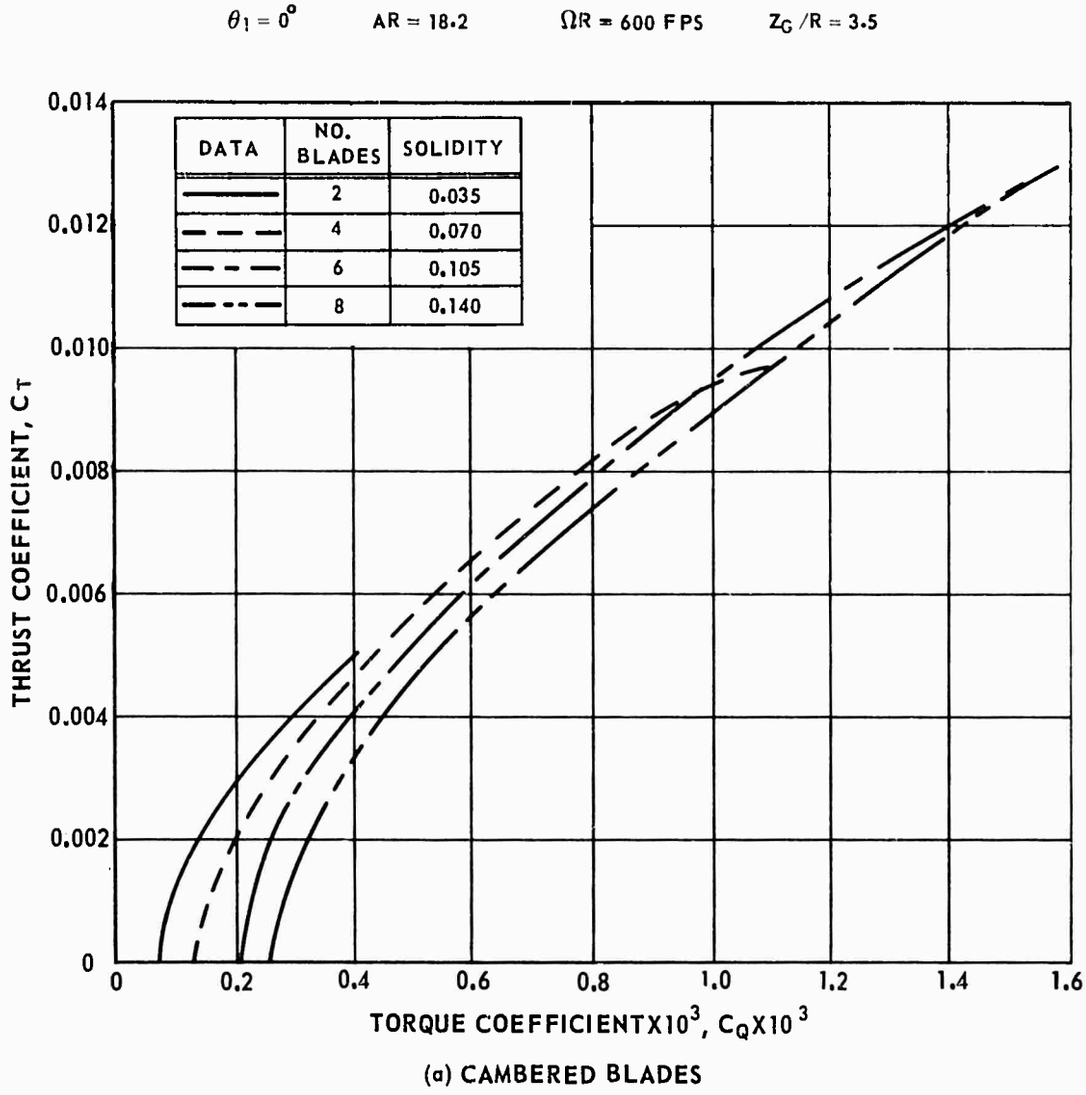

Figure 12. Experimental Model Rotor Hover Performance Expressed in Terms of Thrust and Torque Coefficients.

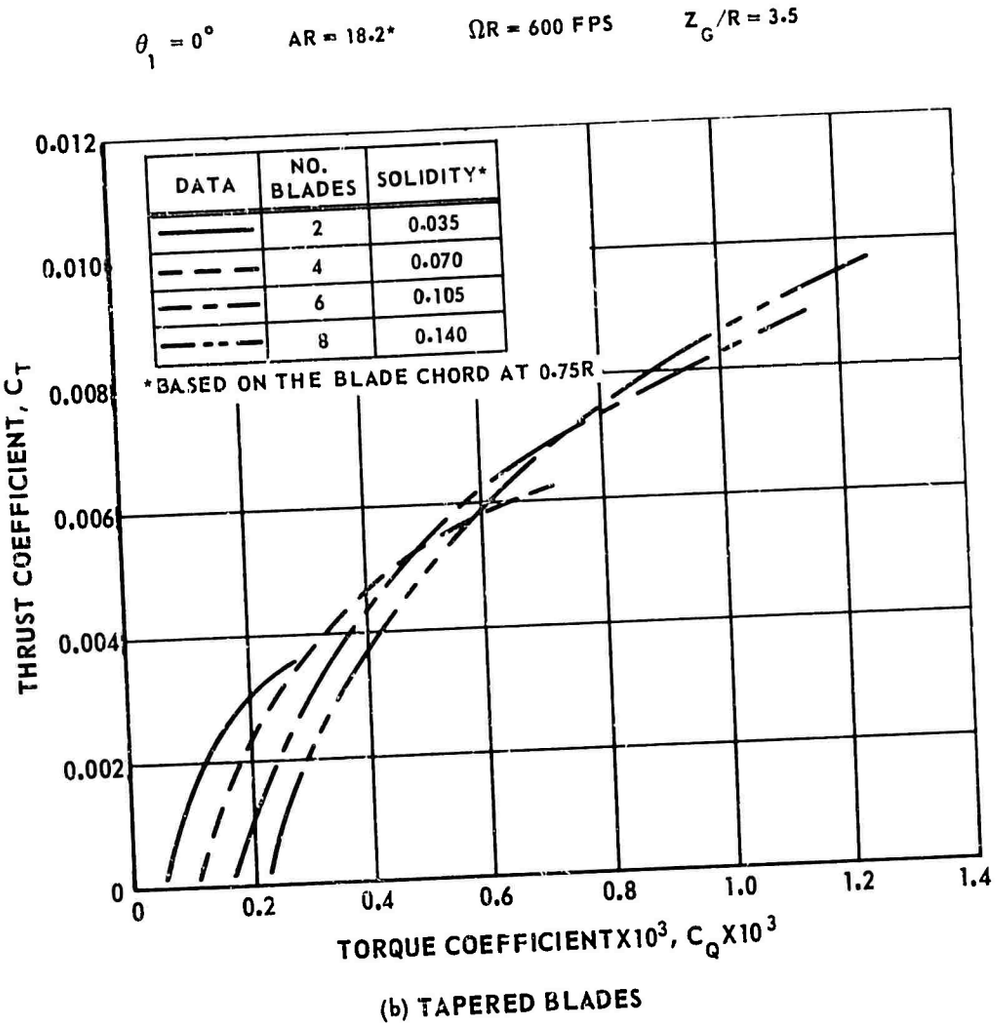

(b) TAPERED BLADES

Figure 12. Concluded.

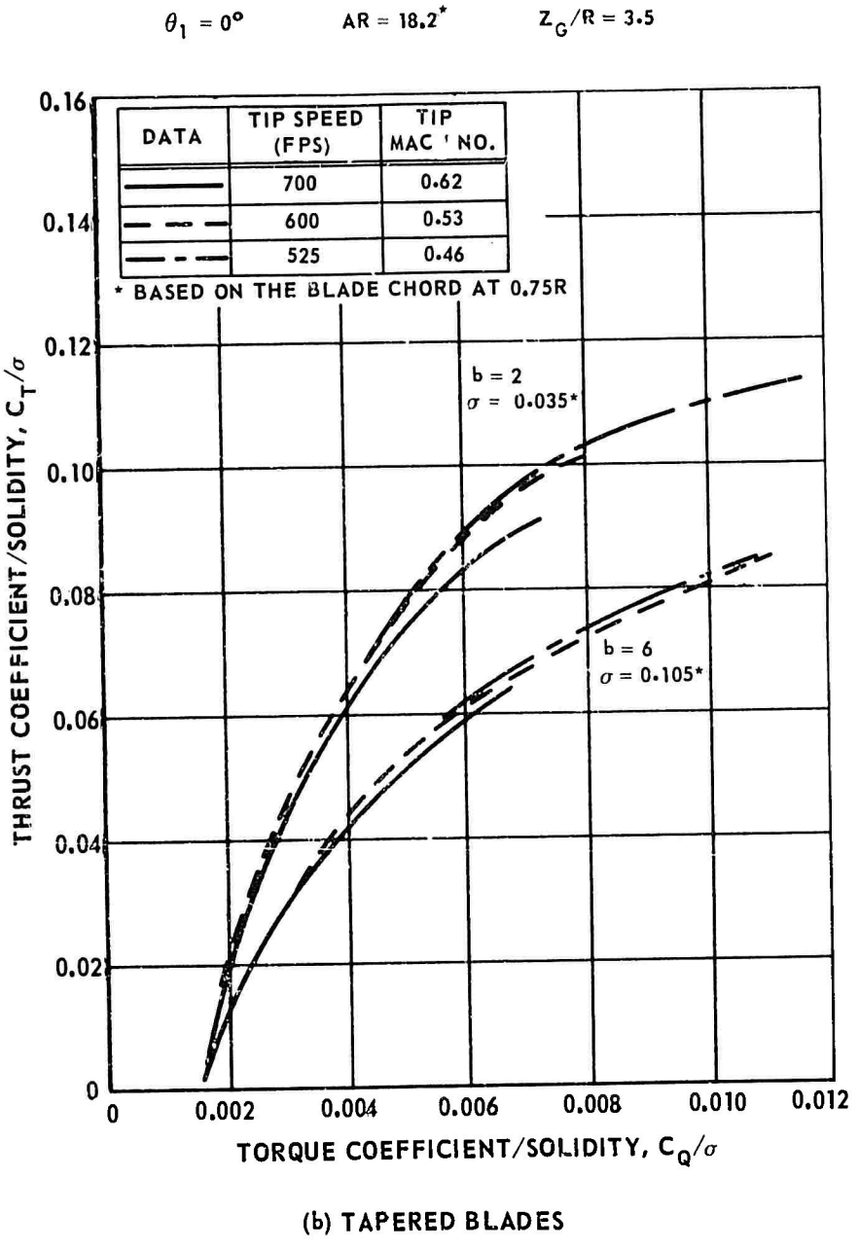

(b) TAPERED BLADES

Figure 13. Concluded.

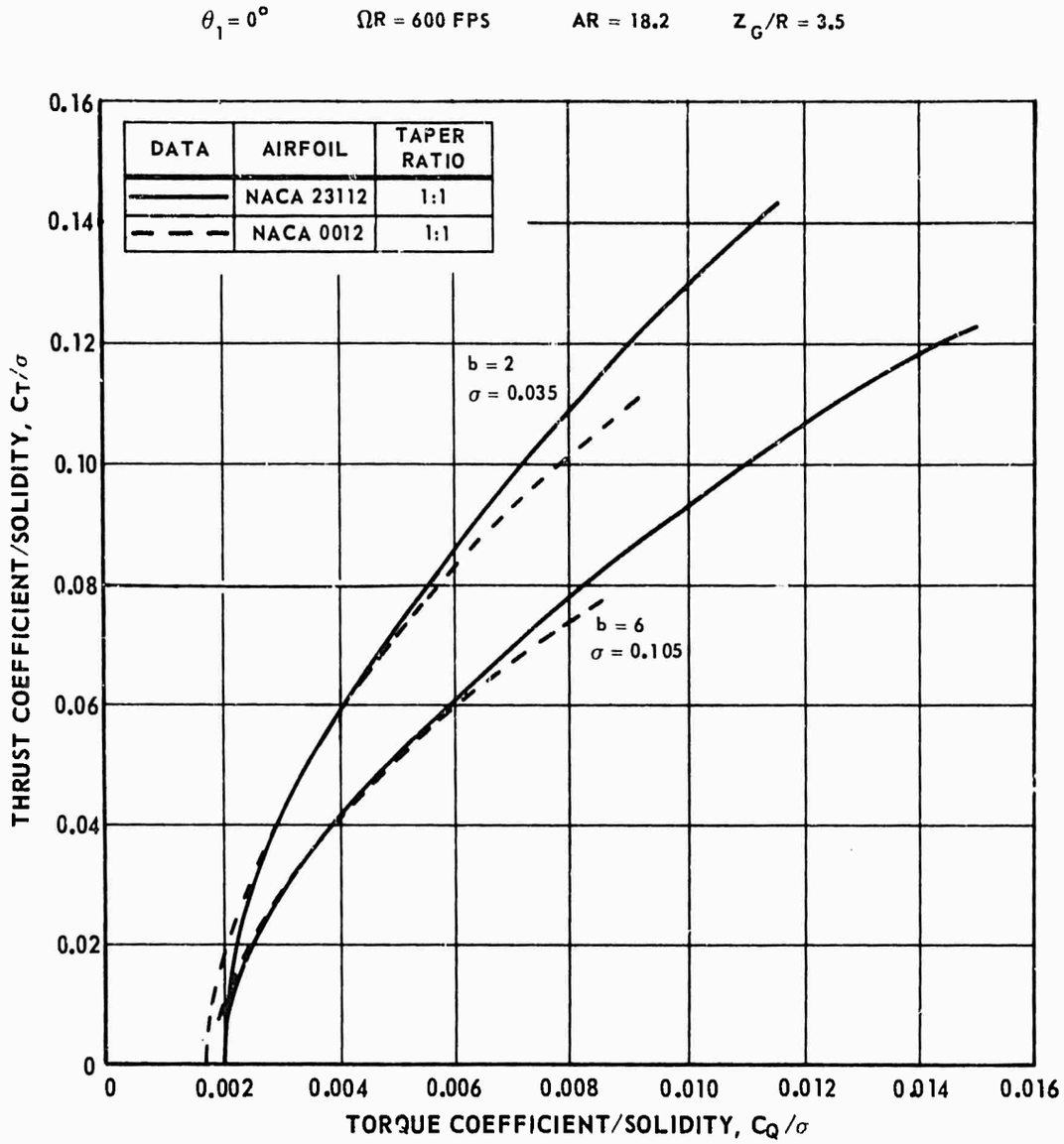

Figure 14. Effect of Blade Section Camber on Experimental Model Rotor Hover Performance.

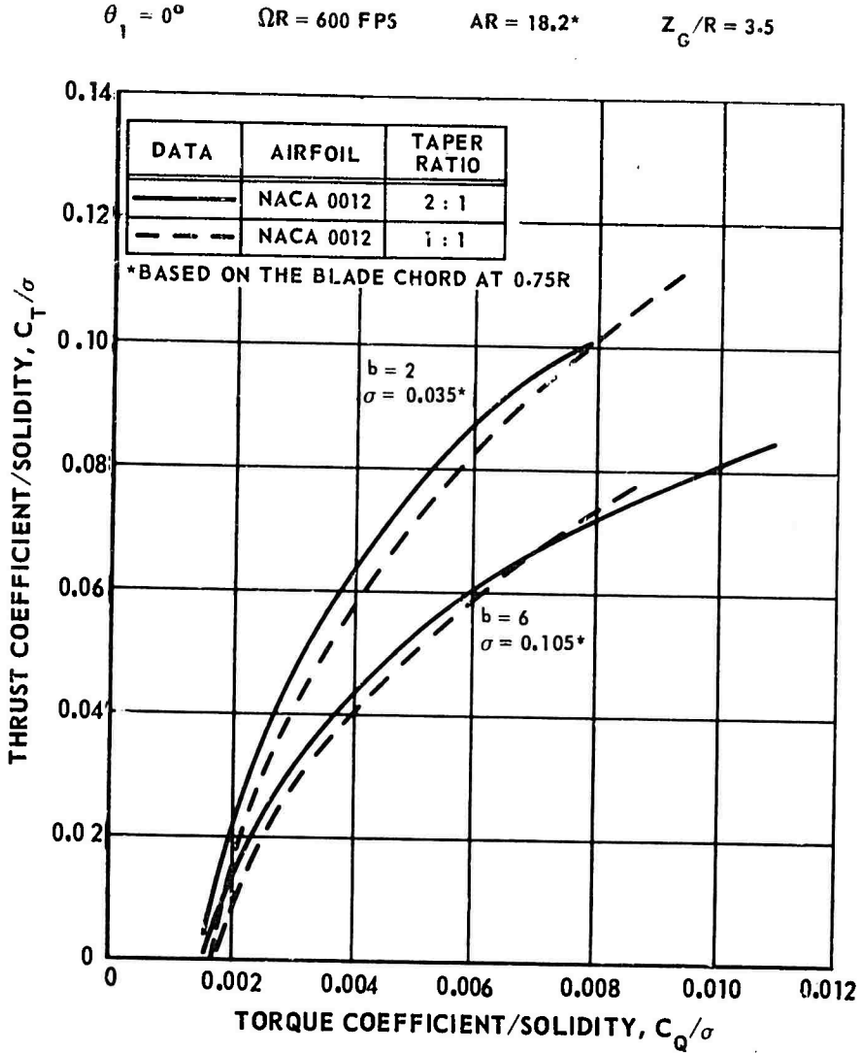

Figure 15. Effect of Blade Planform Taper on Experimental Model Rotor Hover Performance.

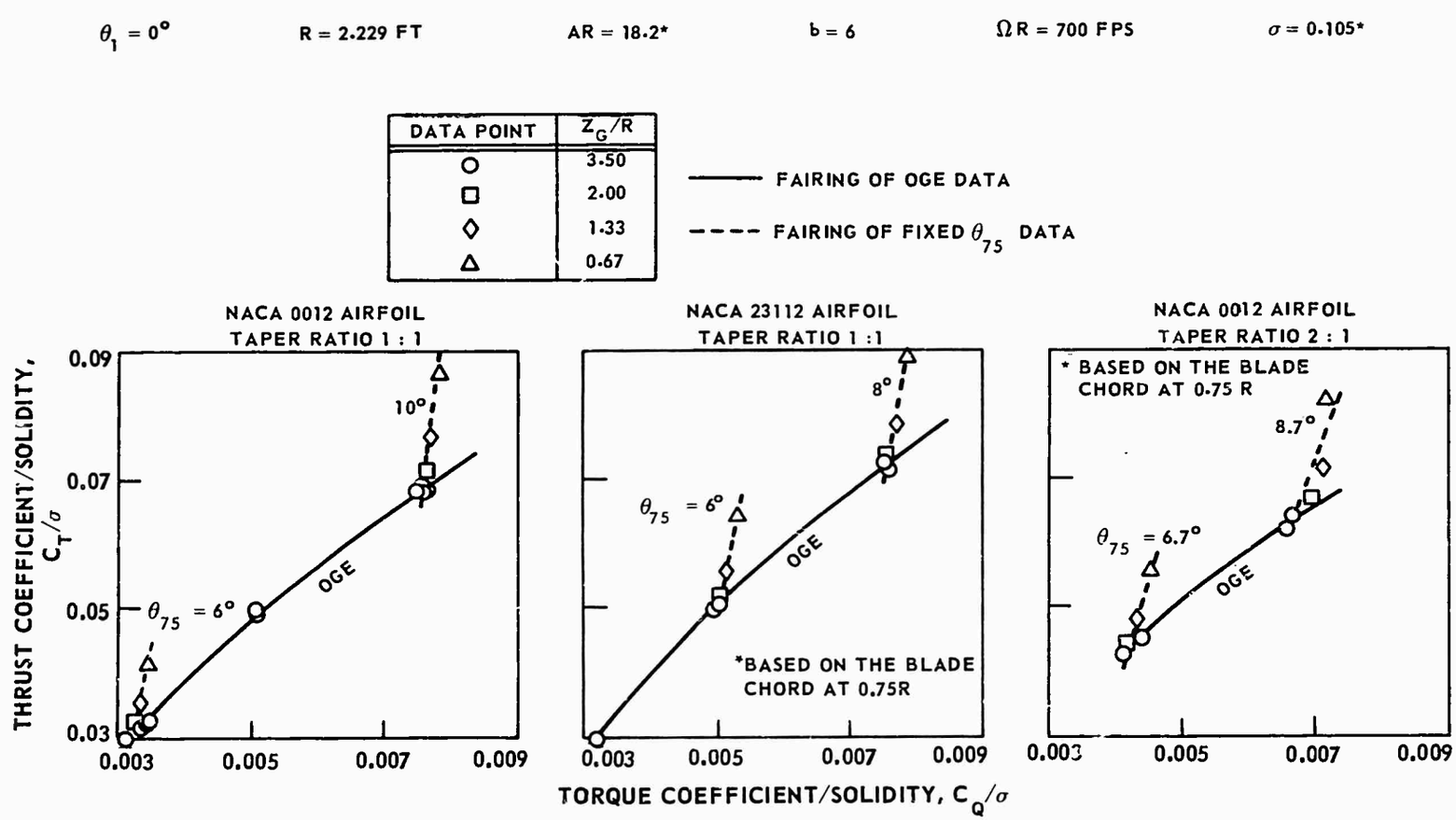

Figure 16. Effect of Rotor Height Above the Ground on Experimental Model Rotor Hover Performance.

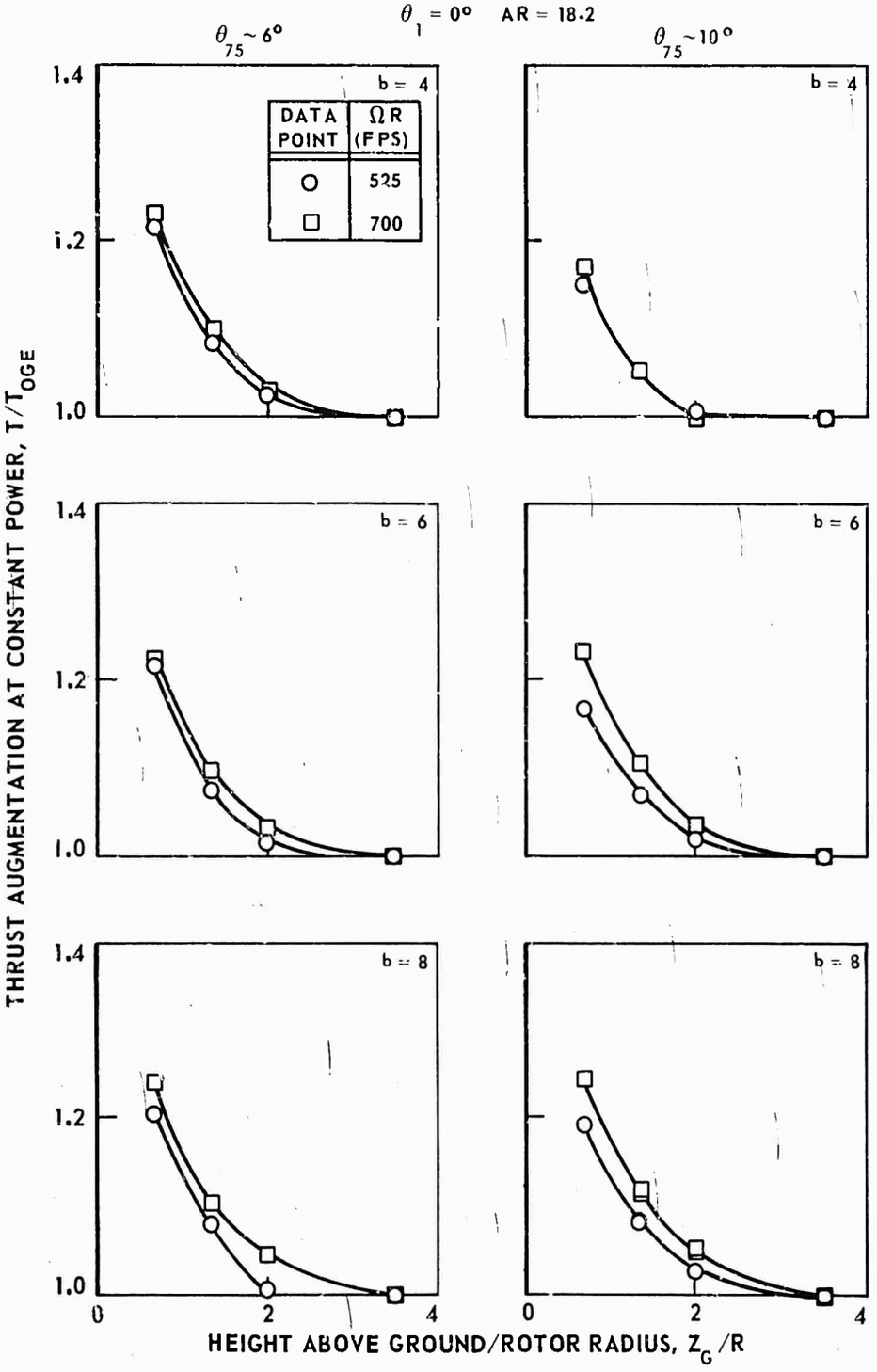

(a) UNTAPERED, SYMMETRICAL BLADES

Figure 17. Experimental Model Rotor Thrust Augmentation due to Rotor Height Above the Ground.

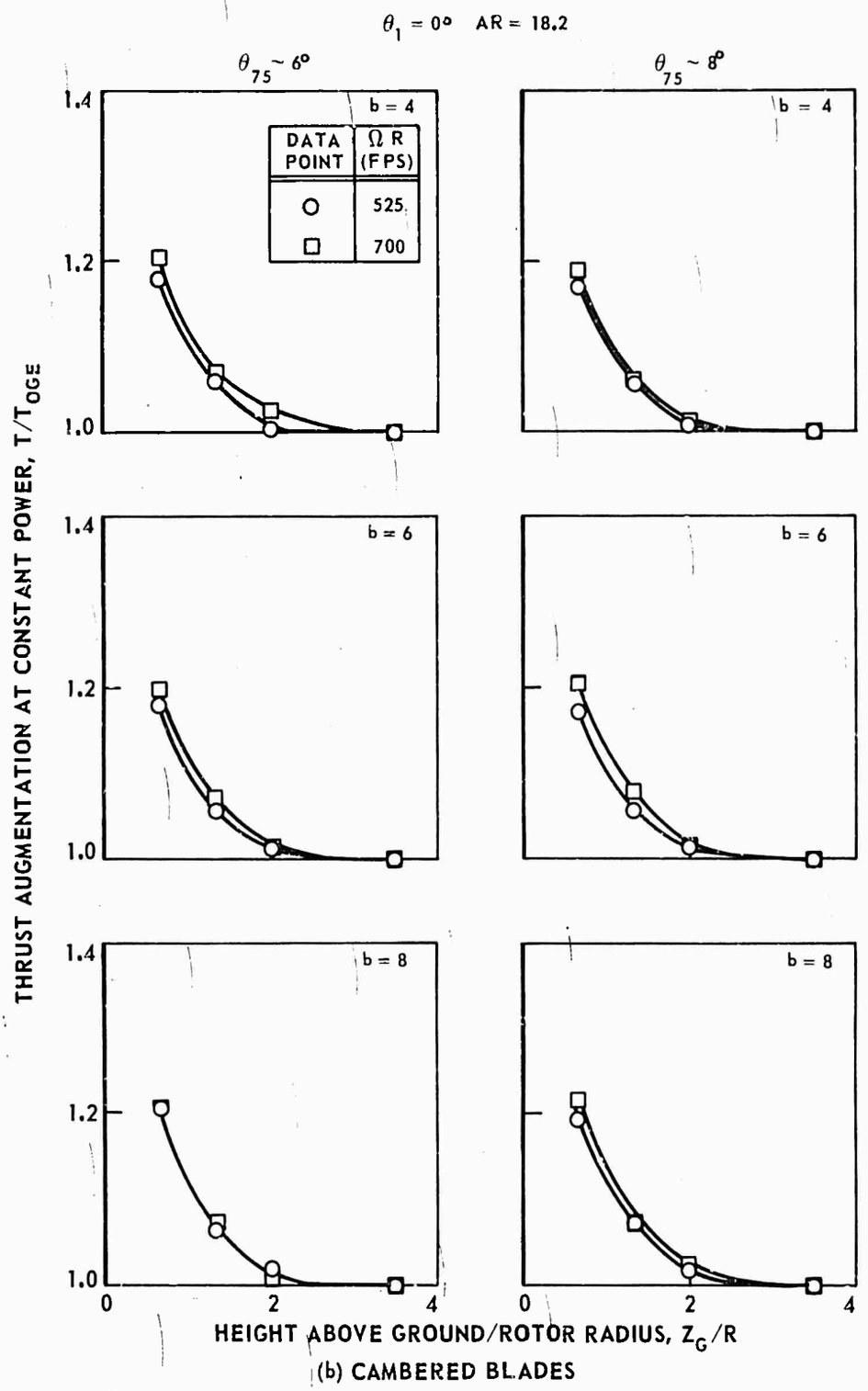

(b) CAMBERED BLADES

Figure 17. Continued.

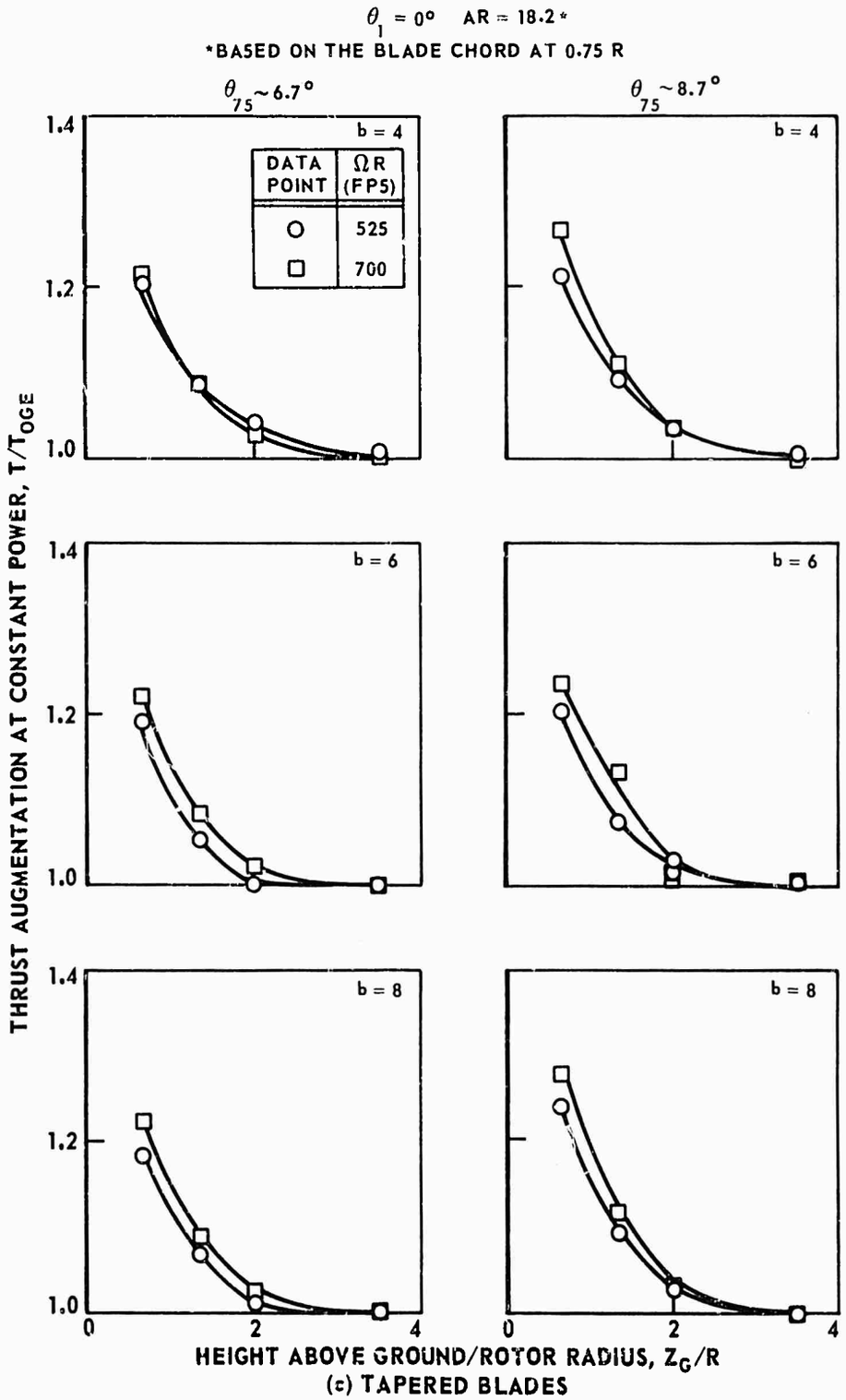

Figure 17. Concluded.

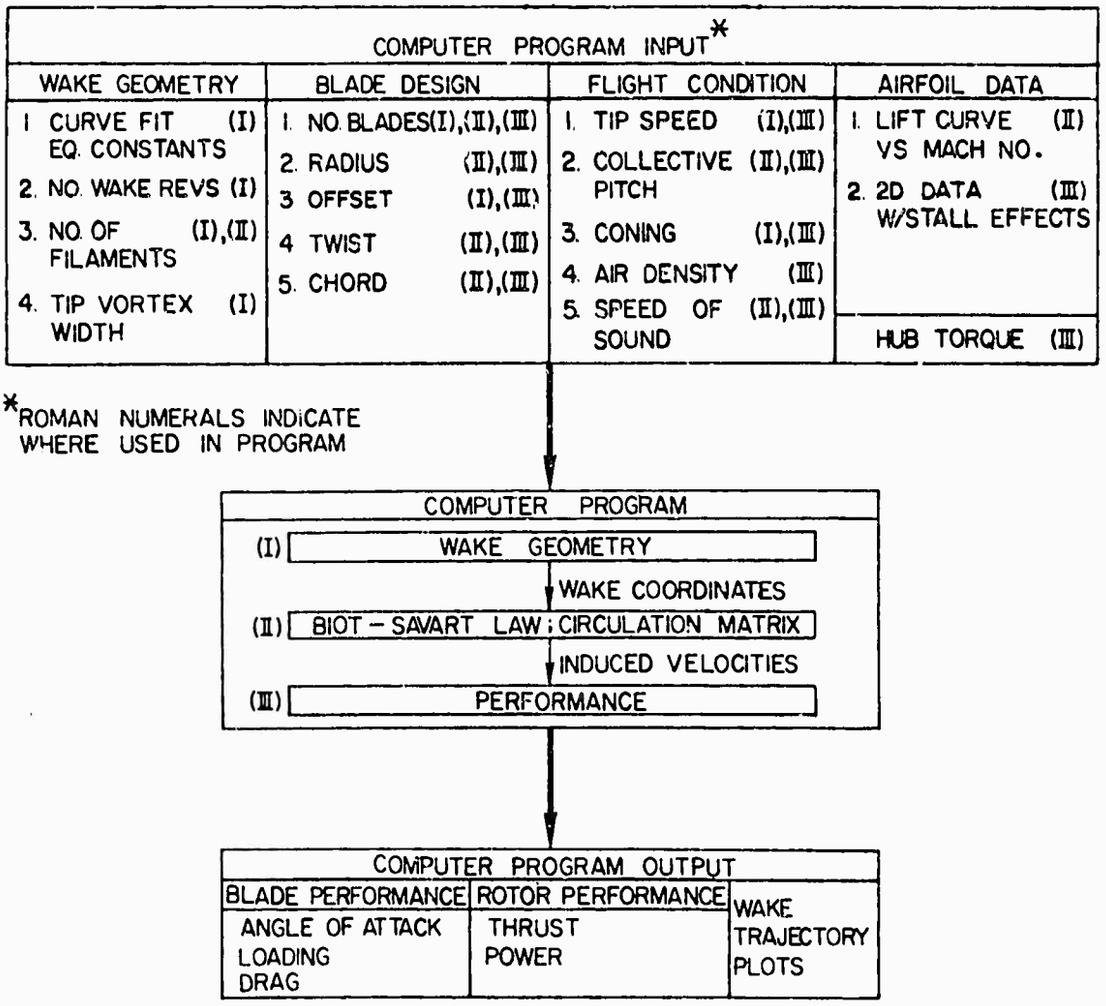

Figure 18. UARL Prescribed Wake Hover Performance Program.

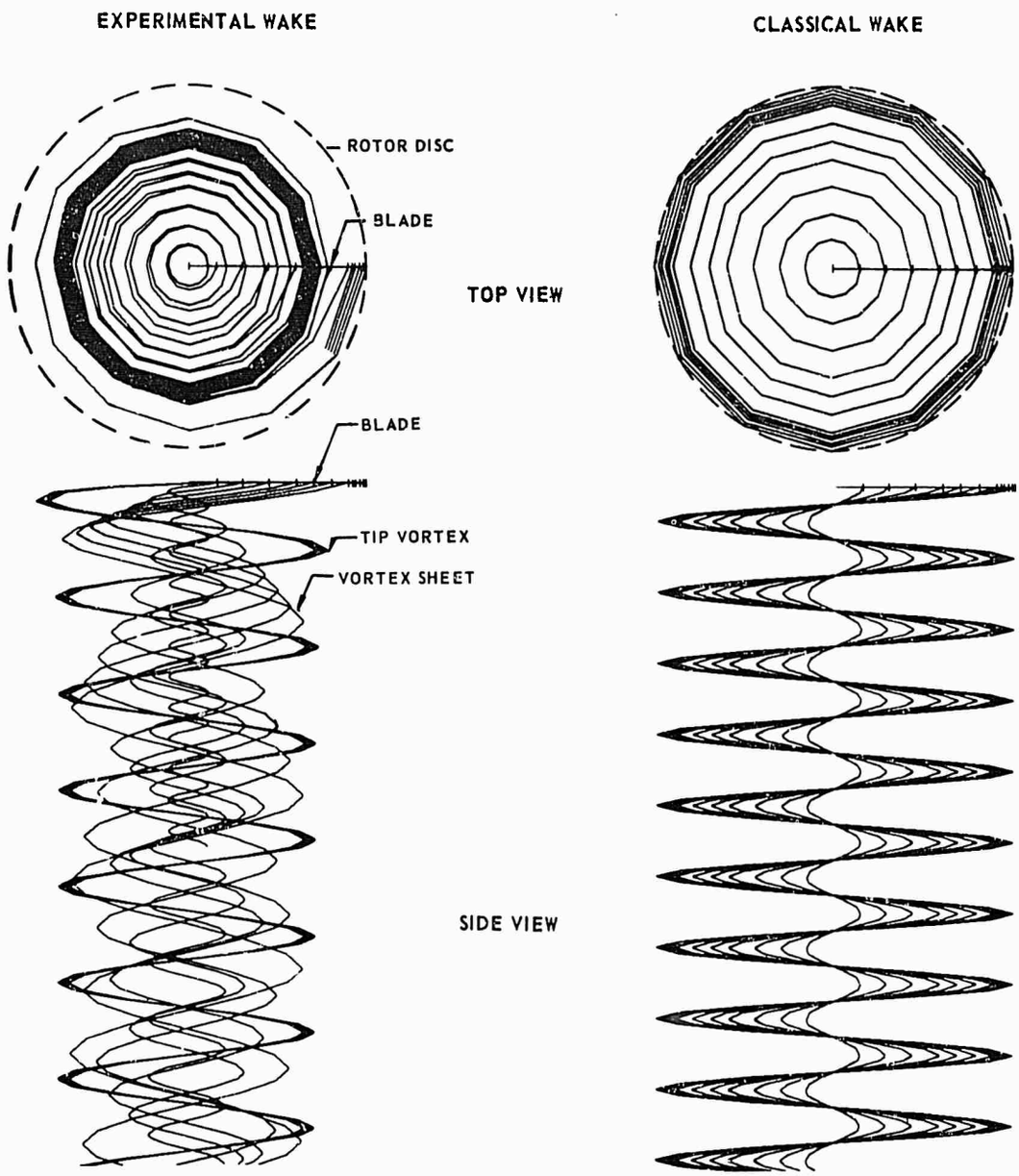

Figure 19. Computer Wake Trajectories for One Blade.

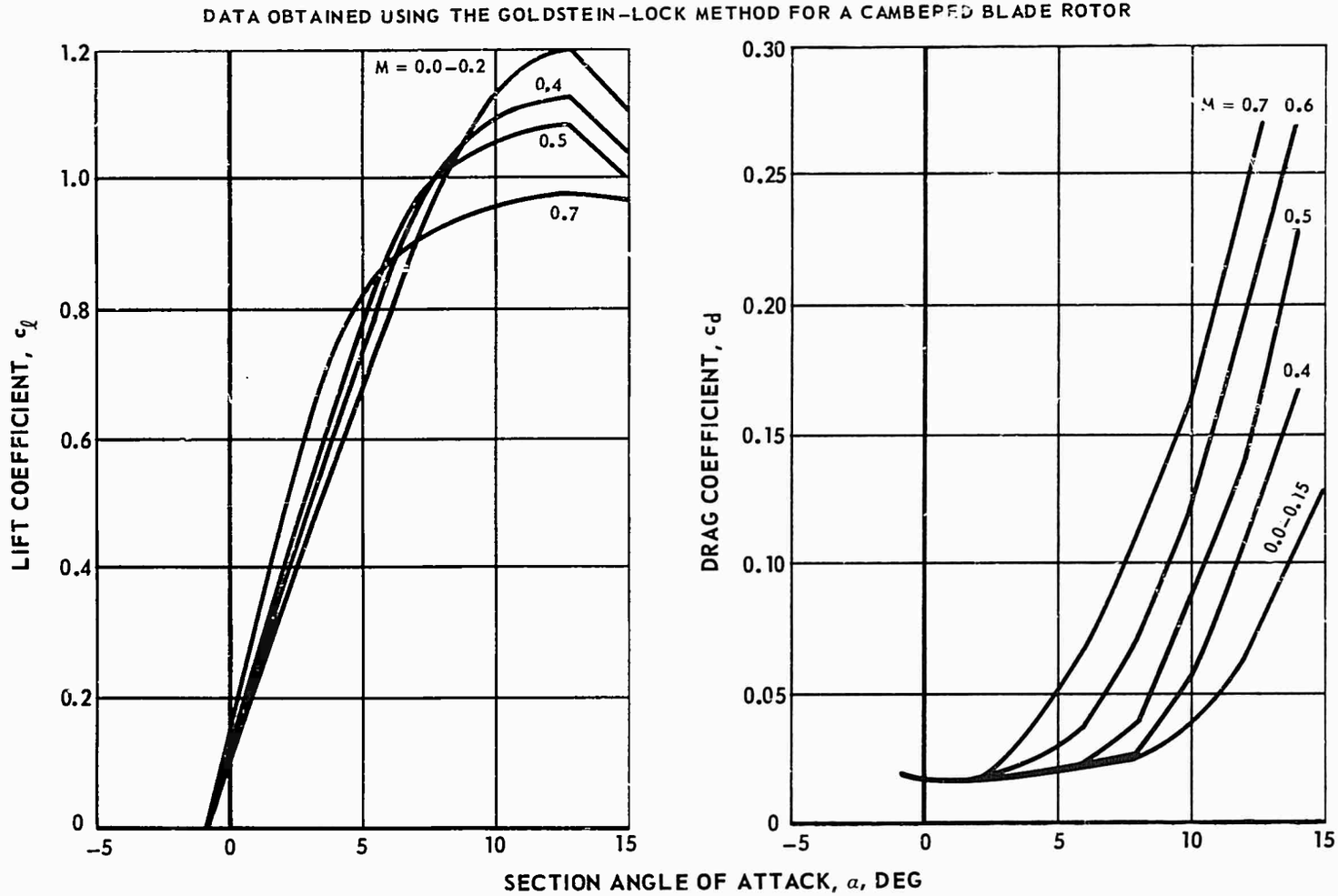

Figure 20. Synthesized Model Rotor NACA 23112 Two-Dimensional Airfoil Data.

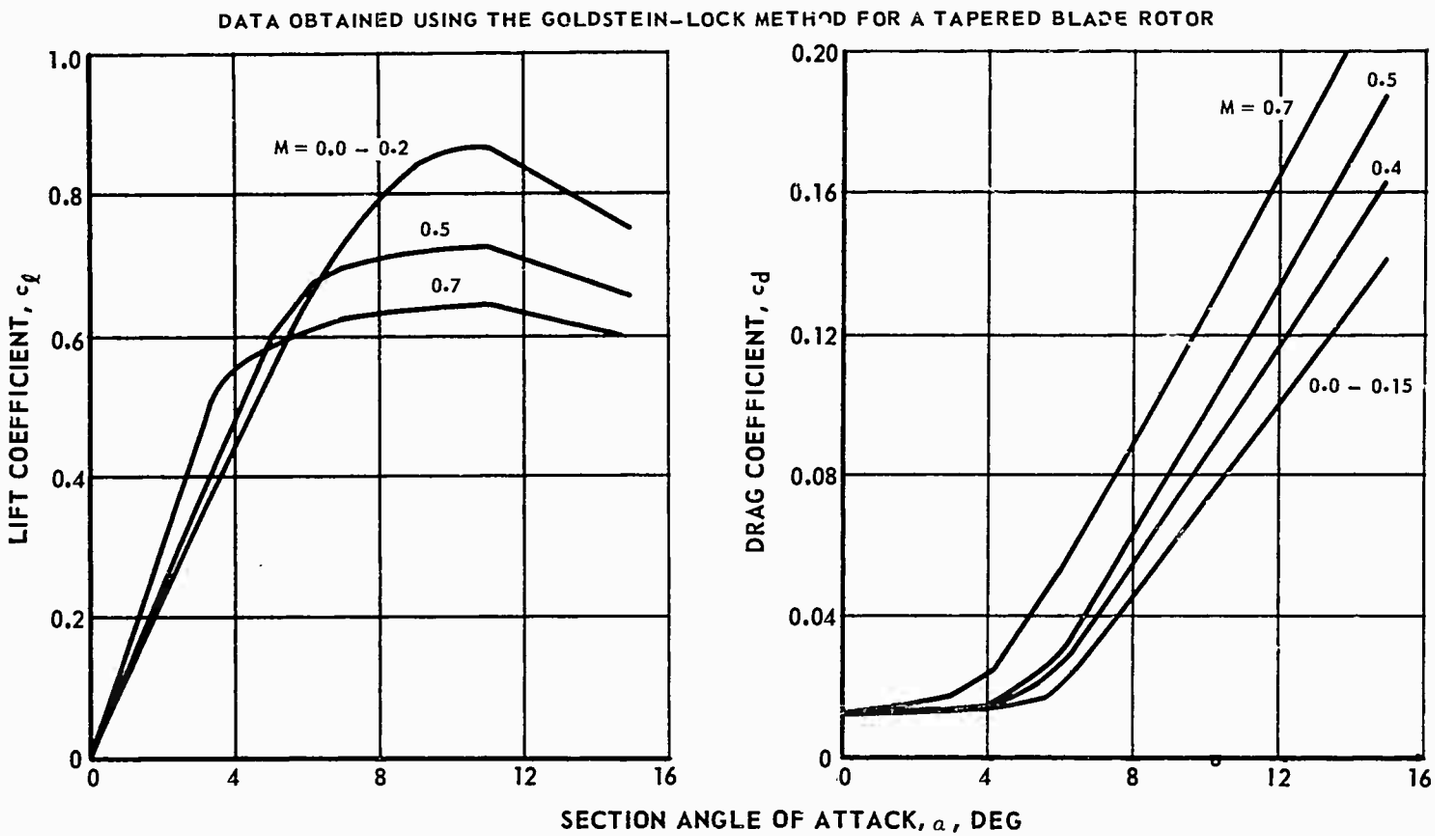

Figure 21. Synthesized Model Rotor NACA 0012 Two-Dimensional Airfoil Data.

$\theta_1 = 0°$ R = 2.229 FT AR = 18.2 $Z_G/R = 3.5$ b = 6 ΩR = 600 FPS $\sigma = 0.105$

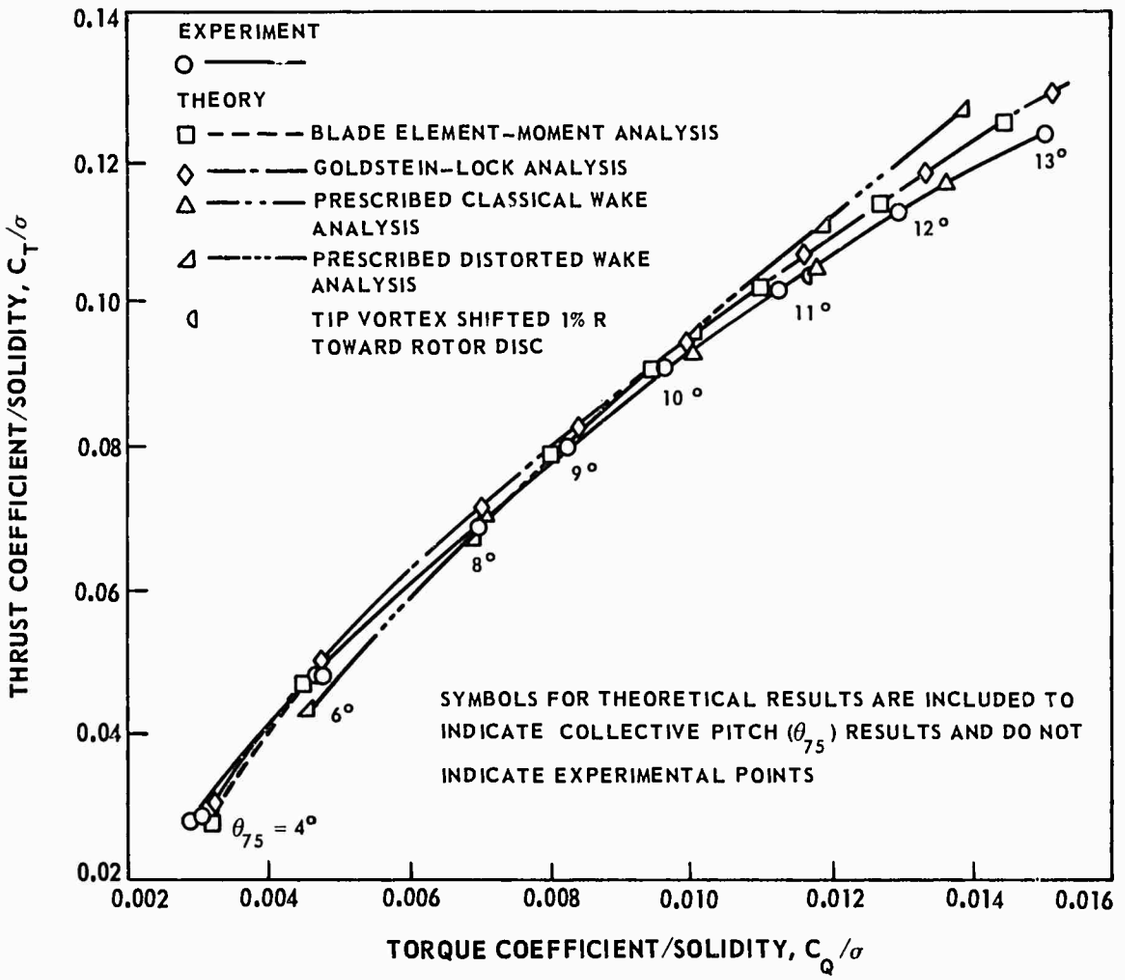

Figure 22. Comparison of Results of Theoretical Analyses With Experimental Hover Performance for Model Scale Rotor Blades With a NACA 23112 Airfoil Section.

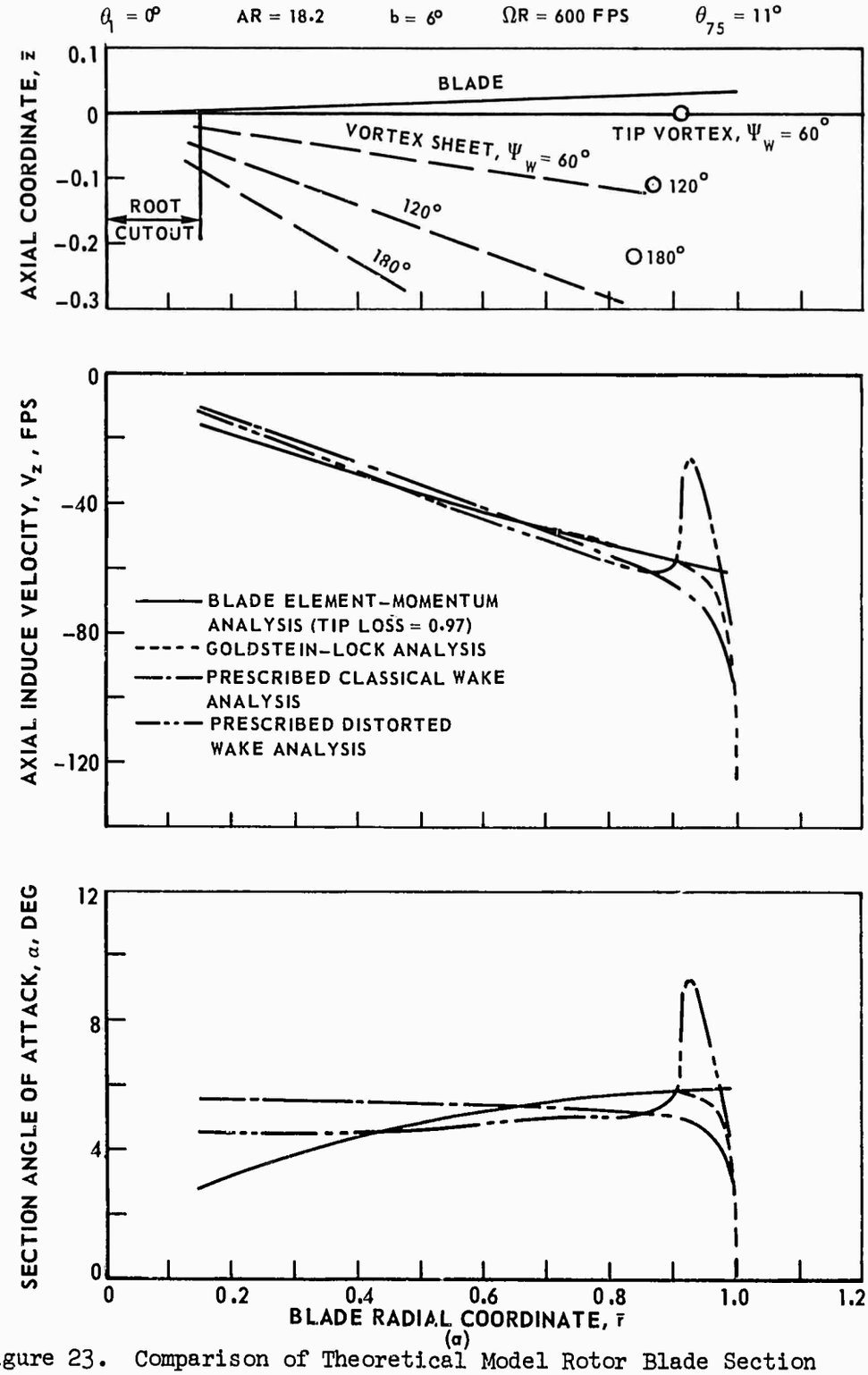

(a)

Figure 23. Comparison of Theoretical Model Rotor Blade Section Characteristics for Blades With NACA 23112 Airfoil Section.

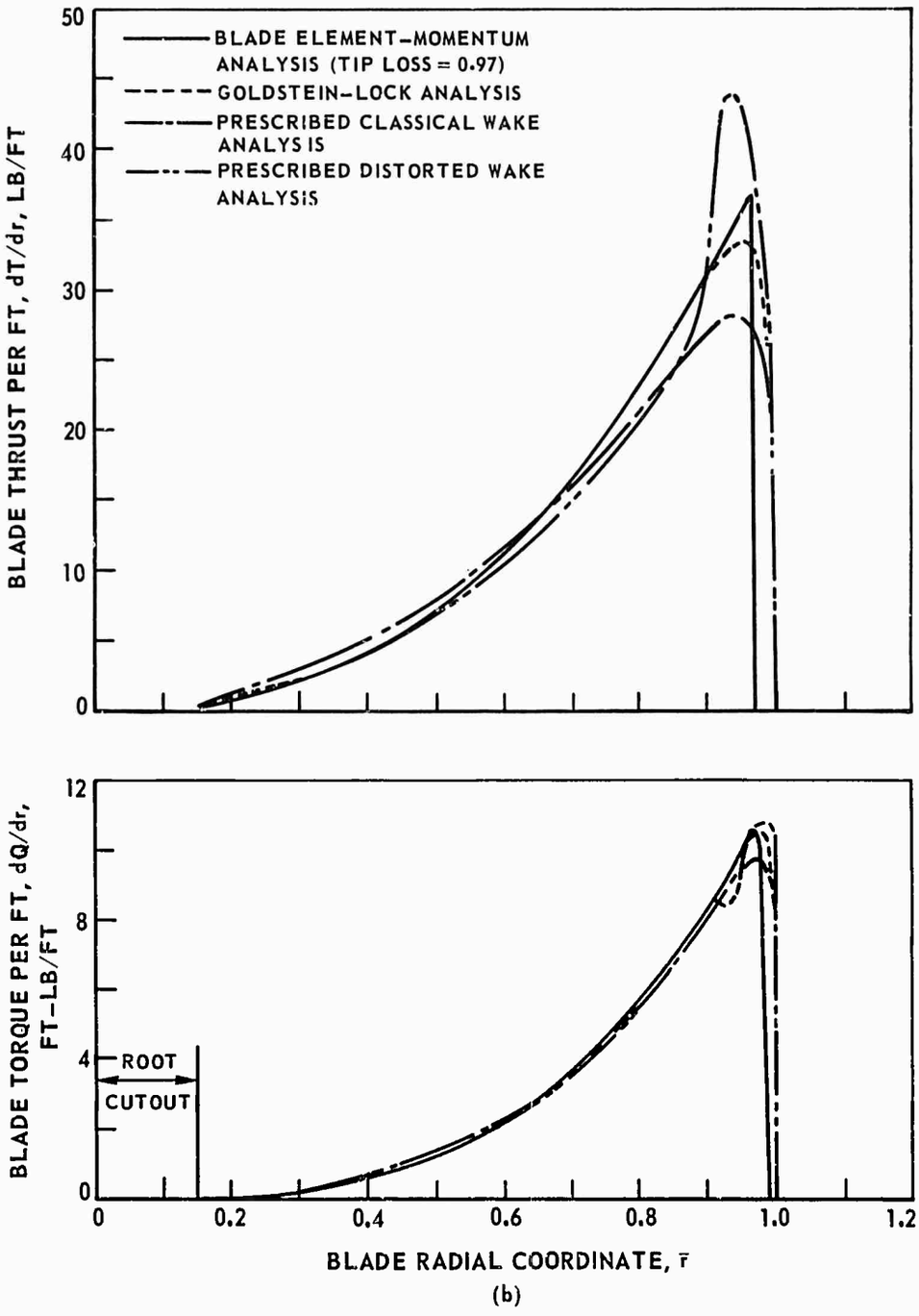

(b)

Figure 23. Continued.

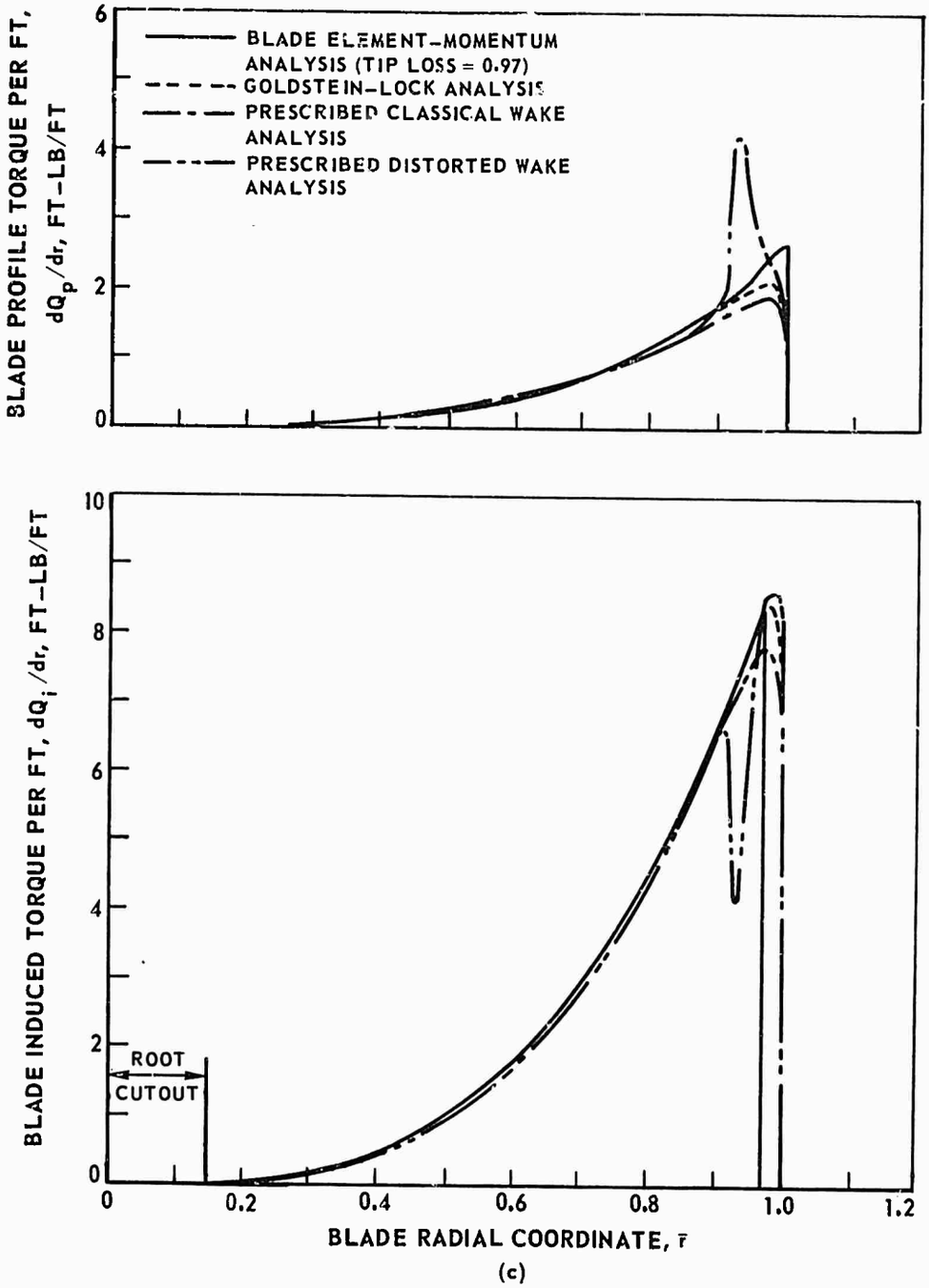

Figure 23. Concluded.

$\theta_1 = 0°$ R = 2.229 FT AR = 18.2* Z_G/R = 3.S b = 6 ΩR = 600 FPS σ = 0.105*

*BASED ON THE BLADE CHORD AT 0.75 R

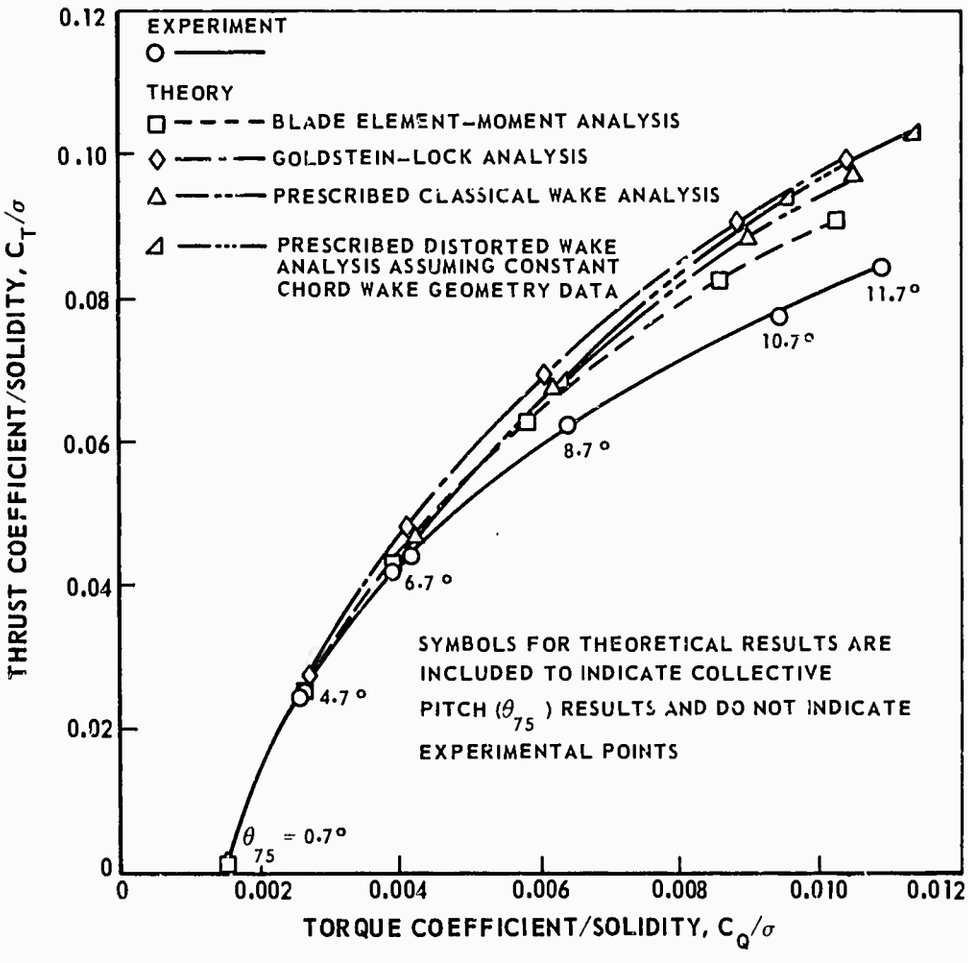

Figure 24. Comparison of Results of Theoretical Analyses With Experimental Hover Performance for Model Scale Rotor Blades With a 2:1 Taper Ratio.

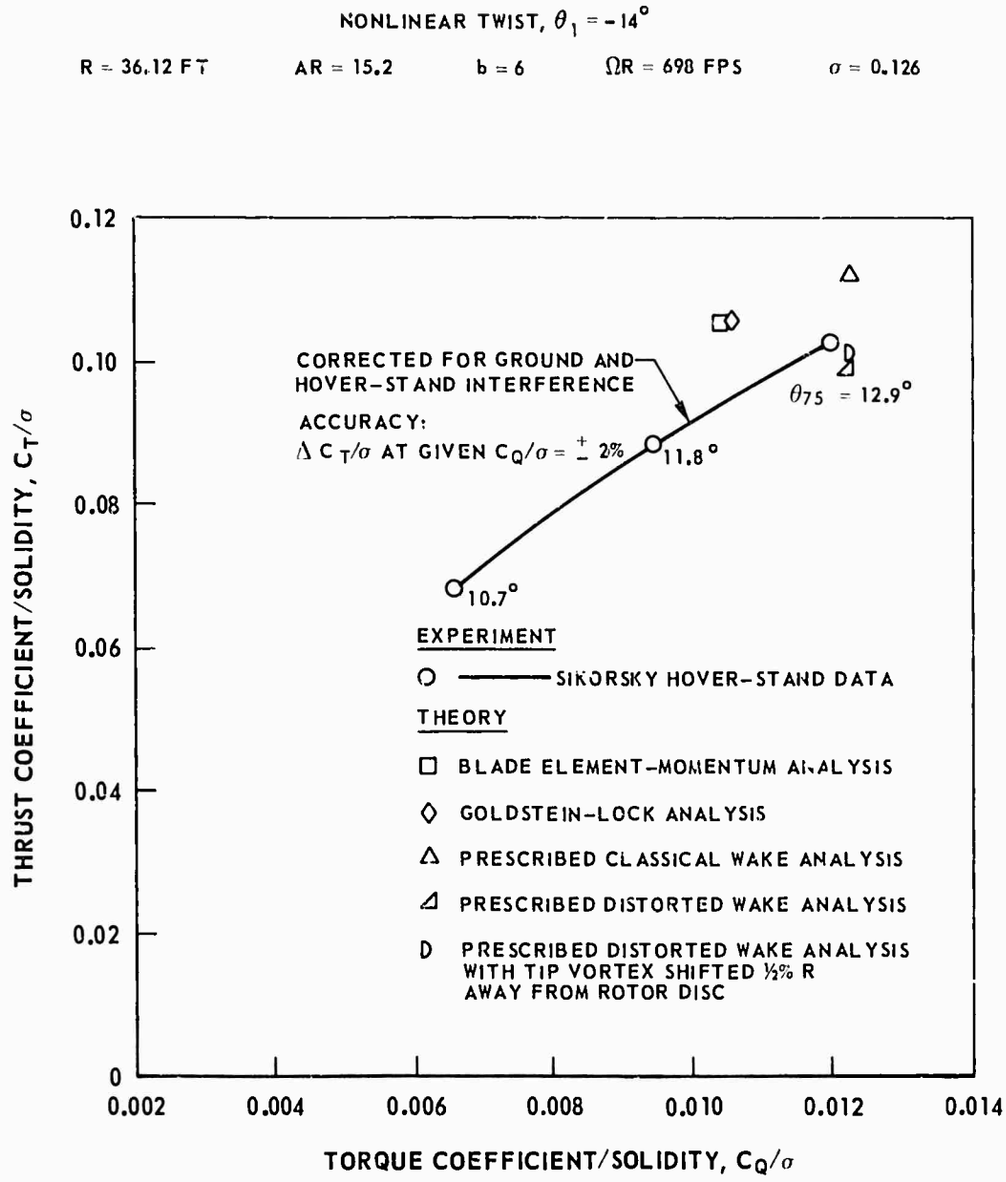

Figure 25. Comparison of Results of Theoretical Analyses With Experimental Hover Performance for Full-Scale Rotor Blades With a Cambered Airfoil Section.

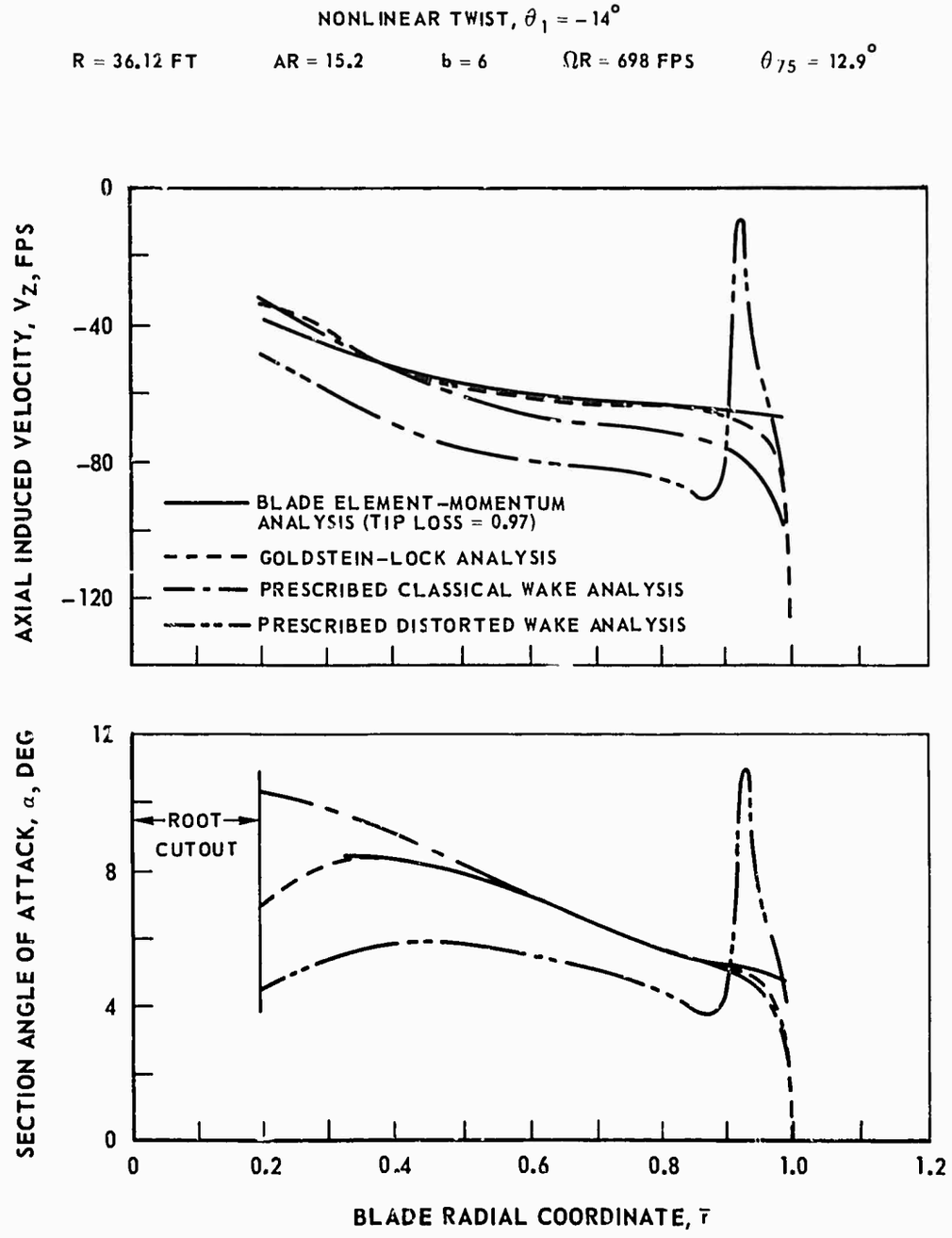

Figure 26. Comparison of Theoretical Full-Scale Blade Section Characteristics for Blades With Cambered Airfoil Section.

LITERATURE CITED

1. Landgrebe, Anton J., AN ANALYTICAL AND EXPERIMENTAL INVESTIGATION OF HELICOPTER ROTOR HOVER PERFORMANCE AND WAKE GEOMETRY CHARACTERISTICS, United Aircraft Corporation; USAAMRDL Technical Report 71-24, Eustis Directorate, U. S. Army Air Mobility Research and Development Laboratory, Fort Eustis, Virginia, June 1971.

2. Jacobs, Eastman N., and Pinkerton, Robert M., TESTS IN THE VARIABLE-DENSITY WIND TUNNEL OF RELATED AIRFOILS HAVING THE MAXIMUM CAMBER UNUSUALLY FAR FORWARD, Langley Memorial Aeronautical Laboratory, NACA TF No. 537, May 1935.

3. Heyson, Harry H., A NOTE ON THE MEAN VALUE OF INDUCED VELOCITY FOR A HELICOPTER ROTOR, NASA Langley Research Center; NASA TN D-240, National Aeronautics and Space Administration, Washington, D.C., May 1960.

4. Goldstein, S., ON THE VORTEX THEORY OF SCREW PROPELLERS, Proceedings - Royal Society of London, Vol. A 123, No. A 792, 1929.

5. Betz, A., HANDBUCH DER PHYSIK, Vol. 7, Berlin, J. Springer, 1927, pp. 256-259.

6. Lock, C. N. H., THE APPLICATION OF GOLDSTEIN'S THEORY TO THE PRACTICAL DESIGN OF AIRSCREWS, ARC R&M No. 1377, Aeronautical Research Committee, Great Britain, 1931.

7. Rorke, James B., and Wells, Clifford D., THE PRESCRIBED WAKE-MOMENTUM ANALYSIS, United Aircraft Corporation, Sikorsky Aircraft Division, Proceedings of the Third CAL/AVLABS Symposium on Aerodynamics of Rotary Wing and V/STOL Aircraft, Vol. 1, Cornell Aeronautical Laboratory, Inc., Buffalo, New York, June 1969.

8. Jacobs, Eastman N., and Sherman, Albert, AIRFOIL SECTION CHARACTERISTICS AS AFFECTED BY VARIATIONS OF THE REYNOLDS NUMBER, Langley Memorial Aeronautical Laboratory, NACA TR No. 586, June 1936.

9. Loftin, Laurence K., Jr., and Smith, Hamilton A., AERODYNAMIC CHARACTERISTICS OF 15 NACA AIRFOIL SECTIONS AT SEVEN REYNOLDS NUMBERS FROM 0.7×10^6 TO 9.0×10^6, Langley Aeronautical Laboratory, NACA TN 1945, October 1949.

10. Critzos, Chris C., Heyson, Harry H., and Boswinkle, Robert W., Jr., AERODYNAMIC CHARACTERISTICS OF NACA 0012 AIRFOIL SECTION AT ANGLES OF ATTACK FROM 0 DEG TO 180 DEG, Langley Aeronautical Laboratory, NACA TN 3361, January 1955.